

Antioxidants & Redox Signaling

Antioxidants & Redox Signaling: <http://mc.manuscriptcentral.com/liebert/ARS>

GLUTATHIONE IS THE RESOLVING THIOL FOR THIOREDOXIN PEROXIDASE ACTIVITY OF 1-CYS PEROXIREDOXIN WITHOUT BEING CONSUMED DURING THE CATALYTIC CYCLE

Journal:	<i>Antioxidants and Redox Signaling</i>
Manuscript ID:	Draft
Manuscript Type:	Original Research Communication
Date Submitted by the Author:	n/a
Complete List of Authors:	Pedrajas, José; University of Jaén, Biochemistry and Cellular Signaling Group, Dept. Experimental Biology McDonagh, Brian; University of Liverpool, Musculoskeletal Biology Institute of Ageing and Chronic Disease Hernández-Torres, Francisco; University of Jaén, Cardiovascular Research Group, Dept. Experimental Biology Miranda-Vizuete, Antonio; Instituto de Biomedicina de Sevilla (IBiS), Hospital Universitario Virgen del Rocío/CSIC/Universidad de Sevilla González, Raul; University of Córdoba, Biochemistry and Molecular Biology Martínez-Galisteo, Emilia; University of Córdoba, Biochemistry and Molecular Biology Padilla, C. Alicia; University of Córdoba, Biochemistry and Molecular Biology Bárcena, José; University of Córdoba, Biochemistry and Molecular Biology
Keyword:	Free Radicals, Metabolism, Mitochondria, Oxygen, Proteomics, Stress

SCHOLARONE™
Manuscripts

ORIGINAL RESEARCH COMMUNICATION

**GLUTATHIONE IS THE RESOLVING THIOL FOR THIOREDOXIN
PEROXIDASE ACTIVITY OF 1-CYS PEROXIREDOXIN WITHOUT BEING
CONSUMED DURING THE CATALYTIC CYCLE**

**José Rafael Pedrajas^{1a}, Brian McDonagh², Francisco Hernández-Torres^{1b}, Antonio
Miranda-Vizuete³, Raúl González-Ojeda^{4,5}, Emilia Martínez-Galisteo^{4,5}, Carmen
Alicia Padilla^{4,5}, José Antonio Bárcena^{4,5*}**

¹⁾ Biochemistry and Cellular Signaling Group (a) and Cardiovascular Research Group (b), Department of Experimental Biology, University of Jaén, 23071-Jaén, Spain.

²⁾ MRC-Arthritis Research UK Centre for Integrated Research into Musculoskeletal Aging (CIMA), Skeletal Muscle Pathophysiology Research Group, Institute of Ageing and Chronic Disease, University of Liverpool, Liverpool L69 3GA, United Kingdom.

³⁾ Instituto de Biomedicina de Sevilla (IBIS), Hospital Universitario Virgen del Rocío/CSIC/Universidad de Sevilla, 41013 Sevilla, Spain,

⁴⁾ Department of Biochemistry and Molecular Biology, University of Córdoba, 14071-Córdoba, Spain.

⁵⁾ Córdoba Maimónides Institute for Biomedical Research, IMIBIC, 14071-Córdoba, Spain.

ABBREVIATED TITLE: Protective and catalytic role of GSH on 1-Cys Prx.

1
2
3 **ADDRESS FOR CORRESPONDENCE:** Prof. J. A. Bárcena, Department of
4
5 Biochemistry and Molecular Biology, Ed "Severo Ochoa", Pl. 1, Campus de Rabanales,
6
7 University of Córdoba, 14071-Córdoba, Spain. Tel.: +34 947 218590; Fax: +34 957
8
9 218592; e-mail: <ja.barcena@uco.es>
10

11
12
13
14 6,420 words (excl. references and figure legends); 45 references; 6 greyscale
15
16 illustrations; 2 color illustrations: (online 2 and hardcopy 0).
17
18
19
20
21
22
23
24
25
26
27
28
29
30
31
32
33
34
35
36
37
38
39
40
41
42
43
44
45
46
47
48
49
50
51
52
53
54
55
56
57
58
59
60

Abstract

Aims: A three-step catalytic cycle is common to all Peroxiredoxins (Prxs) despite structural and kinetic differences. The second step in 1-Cys type Prxs is a matter of debate since they lack an additional cysteine to play the resolving role as happens with the 2-Cys Prxs. The aim of this study was to elucidate the role of glutathione (GSH) in the thioredoxin dependent peroxidase activity of *Saccharomyces cerevisiae* mitochondrial Prx1p, a 1-Cys type Prx. **Results:** The peroxidatic Cys91 residue of two Prx1p peptides can be linked by a disulfide, which can be reduced by thioredoxin and by GSH ($K_m=6.1 \mu\text{M}$). GSH forms a mixed disulfide with the peroxidatic cysteine spontaneously. Mitochondrial Trx3p deglutathionylates Prx1p without the formation of GSSG, so that GSH is not consumed in the process. The structural unit of native Prx1p is a dimer whose subunits are not covalently linked, but a hexameric assembly of 3 disulfide-bound dimers can also be formed. **Innovation:** GSH is presented as a protective cofactor of Prx1p, which is not consumed during the peroxidase reaction, but provides a robust mechanism as the “resolving cysteine” and efficiently preventing Prx1p overoxidation. GSH exerts these roles at concentrations well below those commonly considered necessary for its antioxidant and redox buffering functions. **Conclusion:** A 1-Cys peroxide scavenging mechanism operates in yeast mitochondria involving an autonomous glutathione molecule and the thioredoxin system, which could be of universal validity. Prx1p is fairly well protected from overoxidation, questioning its role in a “floodgate” mechanism for H_2O_2 signaling.

Introduction

Peroxiredoxins (Prx) are ubiquitous enzymes catalyzing non-heme thiol dependent scavenging of peroxides. They constitute an abundant family of proteins in most organisms, constituted by 6 subfamilies based on structural characteristics (39). Despite structural and kinetic differences, all Prx share the same catalytic cycle based on a conserved active-site cysteine residue, the peroxidatic Cys (C_p) whose function is to directly reduce peroxides. The catalytic cycle can be divided into three steps: 1) peroxidation, 2) resolution and 3) recycling (20). In the first step, C_p-S^{\cdot} is oxidized to a sulfenic acid (C_p-SOH) by the substrate peroxide; in the second step a disulfide is formed between C_p and a second resolving Cys (C_R) provided by either the same protein (2-Cys mechanism) or by another protein or small molecule (1-Cys mechanism). Finally, in step three, recycling occurs by reduction of the disulfide by another protein or small thiol molecule regenerating the free thiols C_p-SH and C_R-SH .

Regarding the second step of their catalytic cycle, Prxs are divided into two groups: 1-Cys and 2-Cys Prxs. In 2-Cys Prxs, the resolving thiol is provided by the very same protein forming an intermolecular or intramolecular disulfide bond. However, 1-Cys Prxs do not have a second cysteine to act as the resolving residue near the peroxidatic cysteine and for this reason different mechanisms involving other proteins or small molecules have been postulated. Therefore, the resolving mechanism in 1-Cys Prxs has been a matter of debate for a long time. We have shown that mitochondrial Trx3p, together with the thioredoxin reductase Trr2p, support the peroxidase activity of the 1-Cys Prx of *Saccharomyces cerevisiae*, Prx1p, *in vitro* (16; 31; 32). This would be expected for a canonical peroxiredoxin mechanism, although evidence indicate that Trx3p is not implicated *in vivo* (16). We have also shown that Grx2p can also support recycling of Prx1p with the compulsory involvement of GSH in the catalytic process

1
2
3 (32). Other proposed mechanisms imply the formation of mixed disulfides with diverse
4
5 proteins like Trr2p (16) or π GST (26).
6
7

8 There are characteristics of methionine sulfoxide reductases (Msrs) that resemble
9
10 those of Prxs described above in some ways. Msrs catalyze the reduction of Met-SO in
11
12 a thiol dependent reaction. The catalytic cycle of group-B (MsrBs) can be divided into
13
14 the same 3 steps of oxidation, resolution and recycling and the members are also
15
16 classified into two groups: 2-Cys and 1-Cys MSRB. As for 1-Cys Prxs, resolution of 1-
17
18 Cys MSRB is an open question. It has been proposed that thioredoxin directly reduces
19
20 the sulfenate formed at C_P (24; 41), thus providing both resolution and recycling.
21
22 Resolution by glutathionylation of C_P and recycling by glutaredoxin has also been
23
24 postulated (40). Thioredoxin was proposed to directly reduce the peroxidatic sulfenic
25
26 acid in *E. coli* BCP (23) and PDI that of human glutathione peroxidase Gpx7 (6).
27
28
29

30 Sulfiredoxins (Srxs) catalyze the ATP-dependent reduction of overoxidized sulfinate
31
32 to sulfenate on the C_P of some Prxs. Recently, a model of 1-Cys sulfiredoxin obtained
33
34 by elimination of the second cysteine of yeast Srx was reported to be efficiently
35
36 resolved and recycled by GSH/Grx/glutathione reductase system (7).
37
38
39

40 In all cases where GSH was involved, it was the ultimate electron donor and was
41
42 consumed stoichiometrically per catalytic cycle. We now report evidence that support a
43
44 thioredoxin-dependent mechanism for 1-Cys Prxs in which glutathione is involved but
45
46 is not consumed, thus playing a catalytic role in the second step of the catalytic cycle.
47
48

49 The relationships of glutathione with Prxs have another aspect as a mechanism for
50
51 regulation of the quaternary structure of Prxs. Glutathionylation of the peroxidatic Cys
52
53 of human PRXD1 converts the decamer to its dimeric structure in parallel with loss of
54
55 its activity as a chaperone (9; 29). It has also been described how glutathionylation of
56
57
58
59
60

1
2
3 type-II Prx from poplar, homologous to human PRXD5 induced the dissociation of non-
4
5 covalently bound dimeric Prx (28).
6
7

8 Some Prxs are sensitive to inactivation by their peroxide substrate by overoxidation
9
10 of C_p to sulfinic (C_p-SO₂H) or sulfonic (C_p-SO₃H) before resolution can take place,
11
12 rendering inactive forms of the enzyme. Evidence suggest that structural features that
13
14 favor overoxidation of some members of the Prx family have been selected for during
15
16 evolution to provide a “peroxide floodgate” to allow for signal transduction at
17
18 concentrations of hydrogen peroxide above resting levels (44). Evidence also suggests
19
20 that Prx overoxidation allows them to function as molecular chaperones (22).
21
22
23

24 In a previous work, we demonstrated that the GSH/Grx2/Glr system could efficiently
25
26 support recycling of Prx1p and that GSH affected the oligomeric state of a form of
27
28 Prx1p (32). In the present study we have employed a form of Prx1p with one single
29
30 cysteine (Cys91) in its sequence, the peroxidatic cysteine, which more properly
31
32 represents the native mitochondrial peroxiredoxin according to evidence on its signal
33
34 peptide (43). We report new data on the properties of Prx1p related to its catalytic cycle
35
36 and subunit interaction that present GSH as a protective cofactor which is not consumed
37
38 during the peroxidase reaction, but provides a fast universal mechanism acting as the
39
40 “resolving cysteine” and efficiently preventing Prx1p from overoxidation.
41
42
43
44
45
46
47
48
49
50
51
52
53
54
55
56
57
58
59
60

Results

1. *Prx1p* belongs to *Prx6* subfamily of peroxiredoxins

Prx1p is a mitochondrial peroxiredoxin coded by the YBL064C ORF of *Saccharomyces cerevisiae*. The full sequence contains 3 cysteine residues at positions 6, 38 and 91 (Fig. 1A). To study the molecular and biochemical properties of *Prx1p* we have produced 3 recombinant forms (Fig. 1A). N21*Prx1p* was designed according to a predicted mitochondrial matrix peptidase cutting-site between Q21 and A22. This protein has 2 cysteines at positions Cys38 and Cys91 and has been used and described before (16; 31; 32). We have also produced a site directed mutated form, N21(S)*Prx1p*, in which Cys38 had been substituted by serine, and a form lacking the first 38 residues, N39*Prx1p*. The later is similar to that employed to study the role of ascorbate as a reductant of peroxiredoxins (27). Actually, the N-terminus of the mature *Prx1p* present in the mitochondrial matrix starts at residue 39 as determined experimentally (43). Hence the mature protein contains only one cysteine, Cys91, and belongs to the 1-Cys group of peroxiredoxins included in the *Prx6* subfamily, according to PREX (<http://www.csb.wfu.edu/prex/>) (39). The functional signature of this subfamily, represented by human PRXD6 is highly conserved in yeast *Prx1* (Fig. 1A). A structural modeling of *Prx1p* using human PRXD6 (PDB, 1prx; (11)) as a template, which shares 48% identity, produced a very reliable model with two different servers, SwissModel (5) (QMEAN4 raw score=0,584, Z-score=-2,81 (4)) and I-TASSER (45) (C-score = 0.78 (36)), where even the side-chains of the consensus active site triad are equally oriented (Fig. 1B). The peroxidatic cysteines of each subunit, which are the only cysteines in *Prx1p*, are $\approx 30\text{\AA}$ apart from each other in the dimeric structure.

2. The peroxidatic cysteines of two *Prx1p* peptides can be linked by a disulfide bond.

1
2
3 Electrophoretic analysis of the three recombinant proteins showed differential
4 behavior depending on the number of cysteines present in the protein. When denatured
5 under reducing conditions, N21Prx1p appears as a band corresponding to a peptide of
6 about 28 kDa (Fig.1C) but under non-reducing conditions behaves as a set of bands of
7 different sizes corresponding to one (28 kDa), two (56 kDa), four (\approx 100 kDa), six, etc.
8 peptides. However, when Cys38 was substituted by serine in N21(S)Prx1p only the
9 bands of 28 and 56 kDa were present under non-reducing conditions and the same held
10 true for N39Prx1p (Fig. 2A). These results indicate that the peroxidatic Cys91
11 establishes a disulfide bond between two Prx1p peptides and that these duplets can bind
12 each other by extra disulfide bridges if Cys38 is present.
13
14
15
16
17
18
19
20
21
22
23
24

25
26 Most of the purified recombinant N39Prx1p protein is in the form of Prx1-Prx1 di-
27 peptide under non-reducing electrophoresis (Fig. 2A), but is converted to the single
28 peptide when denatured under reducing conditions in the presence of β -mercaptoethanol
29 (see Fig. 2), an indication that two N39Prx1p polypeptides are linked together by a
30 disulfide bridge between their Cys91. Interestingly enough, the di-polypeptide is also
31 converted to the single peptide by reduction with GSH at low concentrations (<1 mM)
32 (Fig 2B). The effect of GSH is concentration dependent reaching 50% reduction at
33 around 10:1 GSH:Prx1p ratio under the assay conditions, making it physiologically
34 feasible (Fig. 2A). The complete mitochondrial thioredoxin system composed of Trx3p,
35 Trr2p and NADPH, is also an efficient reductant of the disulfide bond between the
36 unique Cys91 residues of each subunit in N39Prx1p (Fig. 2B, lane 4). However, in the
37 absence of Trx3p, Trr2p alone cannot reduce this Prx1-Prx1 disulfide linkage between
38 the catalytic cysteines (Fig. 2B, lane 5). Other non-physiological reductants like TCEP
39 (Fig.2B, lane 6) can reduce this disulfide bridge but not ascorbate (Fig.2B, lane 7),
40 which had been postulated as a possible universal reductant of peroxidases (27).
41
42
43
44
45
46
47
48
49
50
51
52
53
54
55
56
57
58
59
60

1
2
3 Formation of disulfide bond between two Prx1p peptides is induced by the peroxide
4 substrate. Addition of low concentrations of H₂O₂ to a preparation of N39Prx1p
5 previously reduced with TCEP, regenerated the 56 kDa di-polypeptide (Fig. 2C),
6
7
8
9
10 although the proportion of di-peptide formed was lower at relatively high concentrations
11 of peroxide. However, when the peroxiredoxin was previously reduced with GSH, the
12 di-peptide could not be regenerated under the same oxidative conditions (data not
13 shown). This effect was confirmed by another experimental approach. When a
14 preparation of N39Prx1p reduced by the thioredoxin system was mixed with a peroxide
15 generating system formed by xanthine, XO and SOD, the 56 kDa di-polypeptide was
16 formed with time, as the reducing power of the thioredoxin system was exhausted (Fig.
17 2D). However, when GSH was also added, the formation of the di-peptide was
18 abrogated, even at long incubation periods (Fig. 2E). These results indicate that
19 formation of a disulfide bond between two Prx1p peptides is dependent on mild
20 oxidative conditions that oxidize Cys91 to sulfenic in a proportion of Prx1p peptides,
21 while the rest are still reduced, so that both can react between them to form an
22 intermolecular disulfide.
23
24
25
26
27
28
29
30
31
32
33
34
35
36
37
38

39 In this case, Cys91 would have a dual function both as the peroxidatic C_P, and the
40 resolving C_R, thiol. When the peroxide is generated in the presence of a thioredoxin
41 reducing system, the peptides are kept separated initially, but they eventually bind each
42 other when the reducing power is used up and a mild peroxide flux is on. Abolishment
43 of di-peptide formation by GSH is likely due to glutathionylation of Cys91. These
44 results also suggest that disulfide-linked di-peptide formation could be a way to protect
45 the peroxidatic Cys-91 from overoxidation in the absence of GSH, although this is
46 rather unlikely to occur under physiological conditions.
47
48
49
50
51
52
53
54
55
56

57 *3. Prx1p forms a mixed disulfide with GSH, which Trx3p reduces.*
58
59
60

1
2
3 Evidence that Prx1p is glutathionylated was obtained by Western blot using anti-
4 GSH antibodies and confirmed by mass spectrometry. As shown in Fig. 3A, only the
5 single peptides obtained after treatment of the di-peptide with GSH are reactive towards
6 anti-GSH antibodies, indicating that GSH breaks the disulfide bond between two
7 peptides and keeps bound through a mixed disulfide bond to each peptide. Incubation of
8 glutathionylated Prx1p with the mitochondrial thioredoxin system resulted in a decrease
9 of Prx1p reactivity with anti-GSH antibodies (Fig. 3B) indicating that Trx3p has
10 deglutathionylase activity. Electrophoretic bands of untreated samples of N39Prx1p or
11 treated with β -ME, GSH or TCEP were analyzed by LC-MS/MS upon proteolytic
12 digestion with AspN protease. A glutathionylated form of the Cys91 containing peptide
13 was prominently detected in the band of Prx1p treated with glutathione (Fig. 3C), while
14 the protein reduced with β -ME, had a mixed disulfide between Cys91 and β ME, *e. g.*,
15 “destreak” posttranslational modification (Fig. 3D).
16
17
18
19
20
21
22
23
24
25
26
27
28
29
30
31

32 These results clearly demonstrate that GSH has a high affinity for oxidized Prx1p
33 and forms a mixed disulfide with Cys91 spontaneously, as a means to protect and to
34 resolve the catalytic C_P and that Trx3p can reduce this disulfide.
35
36
37
38

39 *4. Native Prx1p shows different oligomeric states whether it is glutathionylated or*
40 *not.*
41
42
43

44 In a previous study we observed that N21Prx1p, which has 2 cysteines per peptide,
45 behaved as an oligomer of hexameric structure or higher when analyzed by size
46 exclusion chromatography, but behaved as a dimer in the presence of GSH (32). In the
47 present study we have carried out a similar analysis with N39Prx1p, which has only 1
48 cysteine per peptide, after treatment or not with GSH, to confirm the role of cysteines in
49 the oligomerization process. Under non-denaturing conditions the untreated N39Prx1p
50 eluted as a molecule of approximately 150 kDa, which would be consistent with a
51
52
53
54
55
56
57
58
59
60

1
2
3 hexamer (Fig. 4A, chromatogram a). An aliquot of this eluted fraction (F1) appeared as
4
5 a 56 kDa band, corresponding to a di-peptide, when analyzed by non-reducing SDS-
6
7 PAGE (Fig. 4A, inset). When N39Prx1p was glutathionylated by preincubation with
8
9 GSH eluted as a 50-60 kDa protein (Fig. 4A, chromatogram b) corresponding to a
10
11 dimer, but this eluted fraction (F2) resulted in a single band of 28 kDa when analyzed
12
13 by non-reducing SDS-PAGE, corresponding to the size of a single peptide (Fig. 4A,
14
15 inset).

16
17
18
19 These results demonstrate that the structural unit of native N39Prx1p is a dimer
20
21 whose subunits are not covalently linked. However, the subunit peroxidatic cysteine of
22
23 one dimer can form a disulfide bridge with the equivalent cysteine of another dimer
24
25 giving rise to a hexameric assembly of 3 disulfide bound dimers.
26

27 28 *5. Oligomerization state of Prx1p in vivo.*

29

30
31 To check whether the hexamers could be formed *in vivo* or not, cell free extracts of
32
33 yeast were analyzed by size exclusion chromatography (Fig. 4B) and the eluates were
34
35 analyzed by Western blot with anti-Prx1 antibodies (Fig. 4B, inset). In these samples,
36
37 Prx1p was only detected in the fractions corresponding to the dimer and appeared as a
38
39 single peptide by non-reducing SDS-PAGE, indicating that the peptides are non-
40
41 covalently associated physiologically. No Prx1p could be detected in the fractions of the
42
43 eluate corresponding to a 150 kDa molecule.
44
45

46
47 Next we checked whether Prx1p would form disulfide-bridged dipeptides *in vivo*.
48
49 Cell free extracts from mutants of mitochondrial redoxins or glutathione synthetase
50
51 (Δ GSH) were analyzed by non-reducing SDS-PAGE followed by detection of Prx1p by
52
53 Western blot (Fig. 5A). Disulfide bonded peptides could not be detected by SDS-PAGE
54
55 in a Δ GSH mutant lacking γ -glutamylcysteine synthetase or in mutants lacking the
56
57 mitochondrial redoxins Grx2p or Trx3p or both. The di-peptide could not be detected
58
59
60

1
2
3 even in total cell-free extracts or mitochondrial subcellular fractions under different
4
5 oxidative conditions (data not shown). Di-peptides could only be detected in the Δ GSH
6
7 mutant when the cell free extract was dialyzed before loading onto the gel (Fig. 5B).
8
9 This result indicates that a metabolite is necessary to keep Prx1p away from forming an
10
11 inter-subunit disulfide bond in the absence of GSH. From the results presented in Fig.
12
13 2D we postulate that this metabolite should be NADPH acting through the Trx system.
14
15

16 17 *6. GSH stimulates the thioredoxin dependent peroxidase activity of Prx1p.*

18
19 Given two options to resolve the peroxidatic cysteine, either through a disulfide bond
20
21 between two Cys91 of two subunits or by a mixed disulfide with glutathione, it was
22
23 worth comparing their kinetic efficiency when thioredoxin acted as the final thiol
24
25 reductant for the recycling step of the catalytic cycle. As shown in Fig. 6A, reduction of
26
27 peroxide is faster if GSH is present in the reaction mixture than when it is absent and
28
29 the effect is immediate after addition of GSH to the reaction mixture (Fig. 6B). The
30
31 peroxidase activity slows down progressively when GSH is absent, likely due to
32
33 overoxidation under the conditions of the assay, but the reaction rate duplicates when
34
35 GSH is added (Fig. 6B).
36
37

38
39 Since glutathione plays a catalytic role in this reaction, a very small stoichiometric
40
41 concentration of GSH was sufficient to reach maximum activity with a very small Km
42
43 value of 6.1 μ M (Fig. 6C). However, when the final reductant was Grx2, higher
44
45 concentrations of GSH were necessary for maximum activity (Fig. 6D). As expected,
46
47 the activity with Grx2 was highly dependent on GSH concentration, since GSH is also a
48
49 reactant, not just a catalyst. These results demonstrate that the cysteine of glutathione is
50
51 endowed with the highest efficiency ever reported for a resolving C_R of a peroxidase
52
53 system.
54
55

56 57 *7. Structural considerations of Prx1p glutathionylation*

1
2
3 As shown in the first paragraph of this section, the structure of yeast Prx1p can be
4 modeled onto the folding pattern of human PRXD6 with high confidence. We have
5 performed docking simulations of GSH on a model of monomeric Prx1p and on dimeric
6 PRXD6 with SwissDock server with good fitness. A set of poses of docked GSH on the
7 modeled structure of Prx1p are in the vicinity of the active site close enough to react
8 and form a disulfide bond with Cys91 (Fig. 7A). It is worth mentioning the presence of
9 Arg175 at less than 5 Å from Cys91, which could serve as a counterion to stabilize a
10 thiolate during the catalytic cycle, thus explaining the high reactivity of Cys91 with
11 GSH (13).
12
13
14
15
16
17
18
19
20
21
22

23 Peroxidatic cysteine (Cys47) of human PRXD6 lies in the bed of a wide and long
24 groove at the subunits interphase (Fig. 7B and C). Docked GSH fits fairly well in this
25 groove of the dimer with access to the catalytic site (Fig. 7D). In this structure of
26 PRXD6 (PDB: 1PRX) the peroxidatic Cys47 is oxidized in the form of -SOH and the
27 active site is in the fully folded (FF) conformation (20). GSH access to the active site
28 could even improve in the locally unfolded (LU) state needed for the resolution step of
29 the catalytic cycle (20).
30
31
32
33
34
35
36
37
38
39
40
41
42
43
44
45
46
47
48
49
50
51
52
53
54
55
56
57
58
59
60

Discussion

The results shown in Figs. 1C and 2 demonstrate that the Cys91 of two Prx1p peptides can form a disulfide bond between them as a means to carry out the resolving phase of its catalytic cycle and to provide Trx3p with a substrate to act on for regeneration. Formation of this disulfide between peroxidatic cysteines could also serve as a protective mechanism to avoid overoxidation. This uncovers a novel dual role for this residue both as “peroxidatic cysteine” (C_P) and “resolving cysteine” (C_R). In 2-Cys type peroxiredoxins, these roles are played by two different cysteine residues of the same polypeptide (19). In human PRXD6, which is homologous to yeast Prx1p, the catalytic cysteine is “resolved” by heterodimerization with glutathione transferase π GST (26; 34) but this mechanism is unlikely to be operative in yeast because an equivalent transferase is not present in yeast mitochondria (38).

Contrary to previous reports (Greetham & Grant, 2009; Fig 4 therein) Cys38 is not required to form disulfide-stabilized dimers of yeast Prx1p. A basic di-peptide can be established by disulfide linkage between peroxidatic Cys91 from two peptides as demonstrated by the behavior of N21(S)Prx1p and N39Prx1p, which contain only one cysteine residue. Disulfide linked chains of an apparently unlimited number of these basic di-peptides could be formed if Cys38 were present in the peptide (Fig. 1C). However, if the protein possesses only one cysteine, as is the case of mature yeast Prx1p (43), it would not be possible to form higher order disulfide linked oligomers once both Cys91 of two peptides are already involved in a disulfide bond. On the other hand, the homologous human cytosolic PRXD6 has an additional cysteine, which may explain the observation of high molecular weight forms of this protein under low reducing conditions (15).

1
2
3 A summary of the catalytic cycle of Prx1p in the light of the data presented here is
4 shown in Scheme 2A. The ability of Prx1p to form a disulfide between the peroxidatic
5 cysteines, which can be reduced by Trx3p explains the peculiar thioredoxin peroxidase
6 activity of Prx1p, which has not been detected in other 1-Cys-Prxs. Moreover, the
7 disulfide-linked di-peptide can also be broken by reduced glutathione resulting in the
8 glutathionylation of the peroxidatic cysteines, as confirmed by mass spectrometry (Fig.
9 3). We had already postulated the formation of a mixed disulfide between glutathione
10 and peroxidatic cysteine to explain the glutaredoxin-dependent peroxidase activity of
11 Prx1 (32). Mixed disulfides between glutathione and Prx1p or other peroxiredoxins
12 have been detected before by mass spectrometry, but in all cases glutathionylation was
13 forced under non-physiological conditions by incubation with relatively high
14 concentrations of GSSG. In this study, we demonstrate that glutathionylation of Prx1p
15 at its peroxidatic cysteine takes place directly, in a non-enzymatic mode, at very low
16 concentrations of reduced glutathione, compatible with the cellular physiological
17 environment.

18
19
20
21
22
23
24
25
26
27
28
29
30
31
32
33
34
35
36
37 We also confirm that mitochondrial Trx3p catalyzes the deglutathionylation of Prx1p
38 with very high efficiency. The canonical activity of Trxs is the reduction of inter- and
39 intra-molecular protein disulfide bonds, while reduction of protein-glutathione mixed
40 disulfides is essentially carried out by glutaredoxins (8; 21). However, denitrosylating
41 activity of human Trx1 and Trx2 (3) and deglutathionylating activity by h-type Trxs in
42 *A. thaliana* (2) have also been observed. Cytosolic Trx1 and Trx2 from *S. cerevisiae*
43 were also shown to contribute to lowering the general levels of protein glutathionylation
44 although no specific substrates were identified (18). The conformation of Cys91
45 glutathionylated Prx1p, likely in the locally unfolded state (LU) (20), may favor the
46 interaction with Trx3 in the same way as with the disulfide linked Prx1p dimer. The
47
48
49
50
51
52
53
54
55
56
57
58
59
60

1
2
3 wide groove observed in the interface of both subunits could allocate the protrusion that
4 surrounds the active site cysteines of Trx3p (1), resulting in a good fit between both
5
6
7 proteins.
8
9

10 GSH stimulates Trx3p dependent peroxidase activity of Prx1p (Fig. 6). This could be
11 explained simply by the fact that in the presence of GSH each peroxidatic cysteine
12 would be available for catalysis on its own, whereas in the absence of GSH both
13 peroxidatic cysteines have to be involved at the same time in a single catalytic cycle. In
14 other words, the presence of GSH would be equivalent to duplication of the number of
15 active sites. Actually, addition of small amounts of GSH exactly duplicates the activity
16 of Prx1p. The high affinity of GSH for oxidized Cys91 is remarkable, likely as a
17 consequence of a very high reactivity of the Cys91-SOH formed after the first step of
18 the catalytic cycle, since the K_m of GSH is 6.1 μM and the concentration needed for
19 maximum thioredoxin-dependent peroxidase activity is roughly equimolar with the
20 concentration of Prx1p.
21
22
23
24
25
26
27
28
29
30
31
32
33
34

35 It has been reported that certain plant Trxs display atypical active site sequences with
36 altered residues between the two conserved cysteines *e.g.* WCRKC and it was argued
37 that this sequence context allows them to use one single cysteine for a “monothiol”
38 catalytic mechanism with glutathione as a reductant, since replacement of this sequence
39 by the canonical one, WCGPC was sufficient to suppress its capacity to employ GSH
40 (10). We demonstrate here that this is not the case for mitochondrial Trx3p, whose
41 active site sequence is, indeed, WCGPC but displays full activity with GSH as a
42 cofactor. We propose a typical “dithiol” mechanism for Trx3p in this glutathione
43 dependent recycling step of Prx1p involving both cysteines of the catalytic site as
44 depicted in Scheme 2B. This mechanism would be consistent with the low amounts of
45 GSH required for maximum activity (see Fig. 6). If a monothiol mechanism would take
46
47
48
49
50
51
52
53
54
55
56
57
58
59
60

1
2
3 place, a second GSH molecule would be required to regenerate reduced Trx3p(SH)₂,
4
5 GSH would be consumed as a reactant and would be required at higher concentration as
6
7 with the Grx2p system (Fig. 6D).
8
9

10 Formation of a mixed disulfide between Prx1p and Trx3p has been inferred from the
11
12 detection of a ≈65kDa band by non reducing Western blot with anti-Prx1 antibodies in a
13
14 sample of yeast cells containing a *Trx3::C58S* mutation (17). In the dithiolic mechanism
15
16 we propose, Cys55 of Trx3p could form a transient mixed disulfide either with the
17
18 leaving GSH molecule or with Cys91 of Prx1p. Traces of this mixed disulfide Trx3p-S-
19
20 S-Prx1p were detected by MALDI-TOF mass spectrometry of a reaction mixture
21
22 pointing to the likelihood of formation of a mixed disulfide between Prx1 and Trx3
23
24 (Supplementary Figure).
25
26
27

28 Mitochondrial thioredoxin reductase Trr2p cannot support recycling of the Prx1p
29
30 catalytic cycle without the participation of Trx3p as shown in Fig. 6A. However,
31
32 recycling of Prx1p by a system containing Trr2p and GSH in the absence of Trx3p has
33
34 been observed with presumed formation of a mixed disulfide between Trr2p and the
35
36 N21Prx1p, which bears an additional cysteine residue at position 38 (16). This
37
38 discrepancy may be due to the lack of extra cysteine residues in the more physiological
39
40 N39Prx1p that we have used in this study.
41
42
43

44 In the structure of the non-covalently bound dimer of human PRXD6, the peroxidatic
45
46 cysteines of each subunit are very far away from each other (> 30Å) and the same holds
47
48 true for the modeled structure of yeast Prx1p. It seems likely that the covalently bound
49
50 Prx1p di-peptide is formed by “peptide swapping” between two dimers and would
51
52 require a conspicuous conformational change. It appears that a hexameric assembly
53
54 provides the best arrangement to stabilize the new folding pattern of Prx1p di-peptide
55
56 (Fig. 4A). This supramolecular structure is similar to the oligomeric structures of other
57
58
59
60

1
2
3 Prxs endowed with chaperone activity (29). Even if the hexameric structure of Prx1p
4
5 can perform chaperone activity, its existence *in vivo* would require the unlikely
6
7 depletion of glutathione and NADPH from the mitochondrial matrix.
8
9

10 It has been proposed that oxidation of Trx3p induces apoptosis through “caspase-like
11
12 protein” activation (17). Respiratory growth and harsh oxidative conditions, like
13
14 simultaneous deletion of mitochondrial thioredoxin reductase, *TRR2* and glutathione
15
16 reductase, *GLR1* or 3 mM hydrogen peroxide stress, were necessary to achieve a
17
18 significant Trx3p oxidative shift. Interestingly, oxidation of Trx3p required Prx1p,
19
20 indicating that the signal for apoptosis was dependent on Prx1 (17). Now, this
21
22 phenomenon can be explained with detail in the light of the data that we report herein.
23
24 Lack of Trx2p and Glr1p will eventually cut the supply of GSH and the flow of
25
26 electrons from NADPH to Prx1p, which would protect itself by dimerization through a
27
28 disulfide bridge between peroxidatic Cys91. This would put pressure on the demand for
29
30 Trx3p to recycle Prx1p activity until exhaustion of Trx3p(SH)₂. Accumulation of
31
32 oxidized Trx3p and dimeric Prx1p would occur and the pro-apoptotic signaling
33
34 mechanism will be activated. Whether the hexameric assembly of Prx1p dimers could
35
36 take part in this or other processes, as a signaling element would be an interesting
37
38 matter for further research.
39
40
41
42
43

44 Our results demonstrate that multiple surveillance systems look after Prx1p in the
45
46 mitochondria to avoid its inactivation by overoxidation. First, under conditions of high
47
48 reducing power and low peroxide pressure, the Trx3/Trx2 system would keep the
49
50 peroxidatic Cys91 reduced. Second, if Cys91 is sulfenated, as occurs in the first step of
51
52 the catalytic cycle, GSH would react rapidly with it to halt further oxidation. Third, in
53
54 the unlikely event of these two protective mechanisms failing, Prx1p would self-protect
55
56 itself by formation of a disulfide bridge between the peroxidatic cysteines of two
57
58
59
60

1
2
3 molecules. The later would constitute an emergency mechanism that would keep Prx1p
4
5 in a latent but active state, until GSH or Trx3p(SH)₂ could awake it ready for another
6
7 catalytic cycle.
8
9

10 It would appear that mitochondrial Prx1 from *S. cerevisiae* had developed robust
11 mechanisms to resist against peroxide pressure and to avoid overoxidation and
12 inactivation, consisting of a high reactivity of Cys91-SOH towards the omnipresent
13 thiol GSH. In that way, the presence of just small amounts of GSH in the mitochondria
14 would suffice to quickly react with Cys91-SOH and form a mixed disulfide that would
15 protect this cysteine from further oxidation. Resistance to hyperoxidation is a property
16 shared with human mitochondrial PRDX3 (12) and may be a general characteristic of
17 mitochondrial Prxs, although the mechanisms of resistance may differ. A resistant
18 mitochondrial Prx1p would be protected from overoxidation by GSH or eventually by
19 disulfide self-interaction and always ready to scavenge peroxides. As long as reducing
20 power is available to complete the third step of its catalytic cycle, the mitochondrial
21 build-up and spillover of H₂O₂, as the “floodgate hypothesis” postulates (44), would not
22 take place in the presence of Prx1p. NADPH would eventually provide the required
23 reducing power through the glutathione/Grx2 or Trx3/Trr2 systems, which would then
24 be the real limiting factors for H₂O₂ signaling from mitochondria.
25
26
27
28
29
30
31
32
33
34
35
36
37
38
39
40
41
42
43
44
45
46
47
48
49
50
51
52
53
54
55
56
57
58
59
60

Innovation

1-Cys Prx1p from yeast has the peculiarity of using their unique cysteine residue to accomplish the functions of both peroxidatic and resolving cysteine, when GSH is not available. The action of GSH on the thioredoxin dependent peroxidase activity described here for yeast Prx1p reveals a role of this ubiquitous small molecule at concentrations well below those commonly considered necessary for its antioxidant and redox buffering functions, in the same way as is required for iron sulfur cluster assembly (25). Moreover, GSH exerts this function by itself as a cofactor, which is not consumed in the process and is recovered after every catalytic cycle. It would be worth checking whether this phenomenon is a general characteristic applicable to other peroxiredoxins.

Materials and Methods

Materials: NADPH, GSH, GSSG, TCEP, hydrogen peroxide, tert-butyl hydroperoxide, glutathione reductase from baker yeast, xanthine, xanthine oxidase from bovine milk, superoxide dismutase from *E. coli*, lysozyme, DNase I, human plasma thrombin, protease inhibitor cocktail and PMSF were purchased from Sigma, St. Louis, MO. Yeast strains Y10000 (WT), Y11934 (Δ TRR2), Y17097 (Δ GSH1), Y17197 (Δ TRX3), and Y13090 (Δ PRX1) were obtained from Euroscarf collection. Yeast strain MML44 (Δ GRX2) was a kind gift from Prof. E. Herrero, University of Lleida, Spain (35). The strains JR018 and JR024, carrying the double mutations Δ GRX2/ Δ TRX3 and Δ GRX2/ Δ TRR2, were obtained mating MML44 Mata haploid cells with Y17197 Mat α or with Y11934 Mat α , respectively as described elsewhere (32).

Cloning, expression and purification of the recombinant proteins: Cloning into the pET-15b expression vector (Novagen) of the TRR2, TRX3, PRX1 (for the expression of N21Prx1p) and GRX2 genes of *Saccharomyces cerevisiae* was performed as described elsewhere (30; 31; 33). To clone PRX1 gene for the expression of N39Prx1p, two primers (forward: 5'-GGGCATATGAAACAATTCAAACAAAGTGATCAACC-3'; reverse: 5'-GGGGGATCCTTATTTTCGACTTGGTGAATCTTAAATAGG-3') were designed, containing the NdeI and BamHI sites (underlined), respectively. The primers were used to amplify the corresponding fragment from *S. cerevisiae* DNA by PCR with Expand Long Template System (Roche Molecular Biochemicals). The PCR product was cloned into the pGEM-Te Vector System (Promega) and sequenced. The amplified fragment was subcloned into the NdeI/BamHI sites of the pET-15b expression vector, fusing the cloned fragment to a sequence that codes for a polypeptide of 20 amino acids at the N terminus, containing six histidine residues (His-tag) and a thrombin-cleavage site. *E. coli* TOP10 cells (Invitrogen) were transformed with this construct and colonies

1
2
3 of transformed cells were obtained plating on Luria-Bertani medium containing 1 $\mu\text{g/ml}$
4
5 ampicillin.
6

7
8 The expression of the recombinant proteins was performed in cultures of transformed
9
10 *E. coli* BL21-DE cells in LB medium containing 1 $\mu\text{g/ml}$ ampicillin, growing at 37 °C
11
12 until a OD_{600} of 0.5 was attained. Then, the recombinant proteins were induced by
13
14 addition of 0.5 mM isopropyl- β -D-thiogalactoside (IPTG) to the cultures and cells were
15
16 allowed to continue growing at 25 °C overnight. The collected cells were diluted in 20
17
18 mM TrisHCl, pH 8.0, 0.1 M NaCl, 5 mM β -mercaptoethanol, 0.6 mg/ml lysozyme, 1.2
19
20 $\mu\text{g/ml}$ DNaseI. Lysis was performed as described previously (32). Histidine-tagged
21
22 proteins were purified from the extract by chromatography on a TALON™ Metal
23
24 Affinity Resin column (Clontech), and the His-tag was subsequently removed adding 1
25
26 Unit/ml of thrombin to the purified preparations, dialyzed and passed through the
27
28 affinity column again. Purity of the recombinant proteins was checked by SDS-PAGE
29
30 and concentration was determined according to their theoretical extinction coefficients.
31
32

33
34
35 *SDS-PAGE and western blotting:* SDS-PAGE was performed with homogeneous
36
37 10% (w/v) acrylamide gels. Samples were submitted to protein denaturalization at 100
38
39 °C with 2.5 % (w/v) sodium dodecyl sulphate and in the presence or not of 0.715 M β -
40
41 mercaptoethanol. After electrophoresis, proteins were stained with Coomassie Blue or
42
43 transferred to nitrocellulose membrane with a semi-dry electrophoretic transfer system.
44
45 The membranes were processed by the method of Towbin et al. (42). For the detection
46
47 of Prx1p in samples, polyclonal Prx1p-antibodies were used at 1:5000 dilution. The
48
49 Prx1p antibodies were purified from blood serum of immunized rabbits using a column
50
51 of CNBr-activated Sepharose 4B with N39Prx1p coupled following the procedure
52
53 recommended by the manufacturer (GE Healthcare). For the detection of
54
55 glutathionylated proteins, mouse monoclonal anti-GSH (Virogen, Watertown, MA) was
56
57
58
59
60

1
2
3 used at 1:1500 dilution. Membranes were incubated with the primary antibodies
4
5 overnight at 4° C, then washed and incubated with the secondary antibodies, goat anti-
6
7 rabbit (Bio-Rad) for anti-Prx1p detection and goat anti-mouse (Sigma) for anti-GSH.
8
9
10 Chemiluminescent signal was induced using Clarity Western ECL Substrate (Bio-Rad).

11
12 *Activity assays:* Thioredoxin peroxidase activity was determined
13
14 spectrophotometrically by measuring the oxidation of NADPH in a reaction mixture
15
16 containing 250 μ M NADPH, 0.5 mM GSH, 0.5 μ M Trr2p thioredoxin reductase, 5 μ M
17
18 Trx3p thioredoxin, 5 μ M N39Prx1p peroxiredoxin and 1 mM H₂O₂, in 20 mM TrisHCl,
19
20 pH 8, 100 mM NaCl. The glutaredoxin dependent peroxidase activity of the
21
22 peroxiredoxin was also determined spectrophotometrically in a reaction mixture
23
24 containing 250 μ M NADPH, 0.5 mM GSH, 1 Unit/ml of glutathione reductase, 5 μ M
25
26 Grx2p glutaredoxin, 5 μ M N39Prx1p peroxiredoxin and 1 mM *tert*-butyl
27
28 hydroperoxide, in 20 mM TrisHCl, pH 8, 100 mM NaCl. One unit of peroxidase
29
30 activity is defined as the oxidation of 1 μ mol of NADPH/min.
31
32
33

34
35 *Preparation of cell-free extract from yeast and subcellular fractionation:* *S.*
36
37 *cerevisiae* cells grown in YPD medium up to the stationary phase were harvested and
38
39 resuspended in 50 mM TrisHCl, pH 8, 100 mM NaCl, 0.1% v/v Triton X-100, 1 mM
40
41 PMSF, 0.5% (v/v) of protease inhibitor cocktail and 0.5% (w/v) zymolyase 20T
42
43 (USBiological). Cells were lysed by sonication during one hour while immersed in ice
44
45 cold water. Homogenates were clarified by centrifugation at 12,000 x g for 30 minutes.
46
47 Dialysis of cell-free extracts was performed with D-Tube Dialyzer Mini (Novagen) at
48
49 4°C overnight. Protein concentration was determined spectrophotometrically with Bio-
50
51 Rad Protein Assay using BSA as a standard.
52
53

54
55
56 Cells grown as before were also subjected to subcellular fractionation, as described
57
58 previously (14). Spheroplasts were prepared by incubation with zymolyase 20T (5 mg/g
59
60

1
2
3 of cells) in 20 mM potassium phosphate, pH 7.4, containing 1.2 M sorbitol and 10 mM
4
5 EDTA. Spheroplasts were harvested by centrifugation, diluted in 20 mM MES-KOH,
6
7 pH 6.0, 0.6 M sorbitol, 10 mM EDTA and 0.5 mM PMSF, and disrupted in a Dounce
8
9 homogenizer. The mitochondrial fraction was separated by differential centrifugation,
10
11 first at 2,000 x g and then at 12,000 x g. The precipitate corresponding to the
12
13 mitochondrial fraction was diluted in 20 mM HEPES-KOH, pH 6.8, 0.6 M sorbitol and
14
15 10 mM EDTA.
16
17

18
19 *Gel-filtration chromatography:* A Superose 6 HR 10/30 column coupled to an FPLC
20
21 instrument (Biologic Duo Flow, Bio-Rad) was equilibrated with 20 mM Tris-HCl, pH
22
23 8.0, 100 mM NaCl. A 100 μ l sample was loaded for chromatography, which was
24
25 performed at a flow rate of 0.3 ml/min. Samples contained 50 μ M N39Prx1p, incubated
26
27 or not with 1 mM GSH for 30 min at room temperature before loading onto the column.
28
29 Samples of cell-free extracts contained a protein concentration of 2.5 mg/ml. Several
30
31 standard preparations were run to calibrate the column: Blue dextran (2,000 kDa),
32
33 ferritin (450 kDa), alcohol dehydrogenase (150 kDa), BSA (66 kDa) and carbonic
34
35 anhydrase (29 kDa). Absorbance at 280nm after elution was monitored.
36
37
38

39
40 *Mass spectrometry:* Coomassie stained bands of interest from the SDS-PAGE gels
41
42 kept in LCMS water were cut into pieces, destained, dehydrated with acetonitrile and
43
44 dried in a speed vacuum. The reduction-alkylation step was omitted. AspN protease
45
46 (Promega) was reconstituted as indicated by the manufacturer and was added to the
47
48 sliced gel bands in a calculated ratio of 1:100 enzyme to protein in a total volume of
49
50 100 μ l and incubated overnight at 37°C. The resulting digest was processed following
51
52 the manufacturer's protocol, dried in a speed vacuum and frozen. When required, the
53
54 digest was resuspended in 3% acetonitrile, 0.1% TFA and analyzed by LC-MS/MS by
55
56 injection in an ABSciex 5600+ Triple TOF after a 60 min chromatographic gradient. A
57
58
59
60

1
2
3 MS survey scan was acquired followed by MS/MS scan for the 35 more intense
4 detected ions. Files were searched using Mascot search engine against a *S. cerevisiae*
5 database (2015/02/14 6718 sequences and 3,023,940 residues) including glutathione,
6 destreak (corresponding to mercaptoethanol) and carbamidomethyl dynamic
7 modifications. Targeted analysis of the 1-Cys Prx1p peptide containing Cys91,
8 DFTPVCTTEVSAFAKLKPEF, was performed using open source software Skyline
9 (37). The peak areas of [M+1] precursor ions identified as the Cys91 peptide containing
10 either glutathione (2535.1782), destreak (2306.1083) or carbamidomethyl (2287.1315),
11 were used for relative quantification of the oxidation state of Cys91 (37).
12
13
14
15
16
17
18
19
20
21
22
23
24
25
26
27
28
29
30
31
32
33
34
35
36
37
38
39
40
41
42
43
44
45
46
47
48
49
50
51
52
53
54
55
56
57
58
59
60

ACKNOWLEDGEMENTS

This research was supported by grants from the Spanish Ministry of Economy and Competency (BFU2012-32056) and BIO-0216 from the Andalusian Government and by grant UJA2011/12/55 from the Plan of Support for Research, Technological Development and Innovation of the University of Jaén. The work of Carlos Fuentes, Eduardo Chicano and Ignacio Ortea from the Proteomics Facilities of SCAI, University of Córdoba and UCAIB, IMIBIC, which constitute node 6 of the ProteoRed Platform financed by the Spanish ISCIII, is greatly acknowledged.

AUTHORS DISCLOSURE STATEMENT

No competing financial interests exist.

ABBREVIATIONS

Grx or GRX, glutaredoxin; Msr or MSR, methionine sulfoxide reductase; β ME, β -mercaptoethanol; N21Prx1p and N39Prx1p recombinant Prx1p devoid of a 21 and 39 residues N-terminal signal peptide, respectively; N21(S)Prx1p same as N21Prx1p in which Cys38 has been substituted by Serine; Prx or PRX, peroxiredoxin; *t*-BuOOH, *tert*-buthyl hydroperoxide; Srx or SRX, Sulfiredoxin; SOD, Superoxide dismutase; TCEP, Tris(2-carboxyethyl)phosphine; Trr or TRR, thioredoxin reductase; Trx or TRX, thioredoxin; XO, xanthine oxidase.

REFERENCES

1. Bao R, Zhang Y, Zhou C-Z, and Chen Y. Structural and mechanistic analyses of yeast mitochondrial thioredoxin Trx3 reveal putative function of its additional cysteine residues. *Biochimica et biophysica acta*. 1794:716-721, 2009.
2. Bedhomme M, Adamo M, Marchand CH, Couturier J, Rouhier N, Lemaire SD, Zaffagnini M, and Trost P. Glutathionylation of cytosolic glyceraldehyde-3-phosphate dehydrogenase from the model plant *Arabidopsis thaliana* is reversed by both glutaredoxins and thioredoxins in vitro. *The Biochemical journal*. 445:337-347, 2012.
3. Benhar M, Forrester MT, Hess DT, and Stamler JS. Regulated protein denitrosylation by cytosolic and mitochondrial thioredoxins. *Science*. 320:1050-1054, 2008.
4. Benkert P, Biasini M, and Schwede T. Toward the estimation of the absolute quality of individual protein structure models. *Bioinformatics (Oxford, England)*. 27:343-350, 2011.
5. Biasini M, Bienert S, Waterhouse A, Arnold K, Studer G, Schmidt T, Kiefer F, Cassarino TG, Bertoni M, Bordoli L, and Schwede T. SWISS-MODEL: modelling protein tertiary and quaternary structure using evolutionary information. *Nucleic Acids Research*. 42:W252-258, 2014.
6. Bosello-Travain V, Conrad M, Cozza G, Negro A, Quartesan S, Rossetto M, Roveri A, Toppo S, Ursini F, Zaccarin M, and Maiorino M. Protein disulfide isomerase and glutathione are alternative substrates in the one Cys catalytic cycle of glutathione peroxidase 7. *Biochimica et biophysica acta*. 1830:3846-3857, 2013.

- 1
2
3 7. Boukhenouna S, Mazon H, Branlant G, Jacob C, Toledano MB, and Rahuel-
4
5 Clermont S. Evidence that glutathione and the glutathione system efficiently
6
7 recycle 1-cys sulfiredoxin in vivo. *Antioxidants and Redox Signaling*. 22:731-
8
9 743, 2015.
- 10
11 8. Buchanan BB, and Balmer Y. Redox regulation: a broadening horizon. *Annu Rev*
12
13 *Plant Biol*. 56:187-220, 2005.
- 14
15 9. Chae HZ, Oubrahim H, Park JW, Rhee SG, and Chock PB. Protein glutathionylation
16
17 in the regulation of peroxiredoxins: a family of thiol-specific peroxidases that
18
19 function as antioxidants, molecular chaperones, and signal modulators.
20
21 *Antioxidants and Redox Signaling*. 16:506-523, 2012.
- 22
23 10. Chibani K, Tarrago L, Gualberto JM, Wingsle G, Rey P, Jacquot J-P, and Rouhier
24
25 N. Atypical thioredoxins in poplar: the glutathione-dependent thioredoxin-like
26
27 2.1 supports the activity of target enzymes possessing a single redox active
28
29 cysteine. *Plant physiology*. 159:592-605, 2012.
- 30
31 11. Choi HJ, Kang SW, Yang CH, Rhee SG, and Ryu SE. Crystal structure of a novel
32
33 human peroxidase enzyme at 2.0 Å resolution. *Nature Structural Biology*.
34
35 5:400-406, 1998.
- 36
37 12. Cox AG, Pearson AG, Pullar JM, Jönsson TJ, Lowther WT, Winterbourn CC, and
38
39 Hampton MB. Mitochondrial peroxiredoxin 3 is more resilient to hyperoxidation
40
41 than cytoplasmic peroxiredoxins. *The Biochemical journal*. 421:51-58, 2009.
- 42
43 13. Ferrer-Sueta G, Manta B, Botti H, Radi R, Trujillo M, and Denicola A. Factors
44
45 Affecting Protein Thiol Reactivity and Specificity in Peroxide Reduction.
46
47 *Chemical research in toxicology*. 24:434-450, 2011.
- 48
49 14. Glick BS, and Pon LA. Isolation of highly purified mitochondria from
50
51 *Saccharomyces cerevisiae*. *Methods. Enzymol*. 260:213-223, 1995.
- 52
53
54
55
56
57
58
59
60

- 1
2
3 15. Gong S, San Gabriel MC, Zini A, Chan P, and O'Flaherty C. Low amounts
4 and high thiol oxidation of peroxiredoxins in spermatozoa from infertile men.
5 *Journal of andrology*. 33:1342-1351, 2012.
6
7
8
9
10 16. Greetham D, and Grant CM. Antioxidant activity of the yeast mitochondrial 1-Cys
11 peroxiredoxin is dependent on thioredoxin reductase and glutathione in vivo.
12 *Mol Cell Biol*. doi:10.1128/MCB.01918-08, 2009.
13
14
15
16 17. Greetham D, Kritsiligkou P, Watkins RH, Carter Z, Parkin J, and Grant CM.
17 Oxidation of the yeast mitochondrial thioredoxin promotes cell death.
18 *Antioxidants and Redox Signaling*. 18:376-385, 2013.
19
20
21
22 18. Greetham D, Vickerstaff J, Perrone GG, Dawes IW, and Grant CM. Thioredoxins
23 function as deglutathionylase enzymes in the yeast *Saccharomyces cerevisiae*.
24 *BMC biochemistry*. 11:3, 2010.
25
26
27
28 19. Hall A, Karplus PA, and Poole LB. Typical 2-Cys peroxiredoxins--structures,
29 mechanisms and functions. *The FEBS journal*. 276:2469-2477, 2009.
30
31
32
33 20. Hall A, Nelson K, Poole LB, and Karplus PA. Structure-based insights into the
34 catalytic power and conformational dexterity of peroxiredoxins. *Antioxidants
35 and Redox Signaling*. 15:795-815, 2011.
36
37
38
39 21. Holmgren A, Johansson C, Berndt C, Lönn ME, Hudemann C, and Lillig CH. Thiol
40 redox control via thioredoxin and glutaredoxin systems. *Biochemical Society
41 transactions*. 33:1375-1377, 2005.
42
43
44
45 22. Jang HH, Lee KO, Chi YH, Jung BG, Park SK, Park JH, Lee JR, Lee SS, Moon JC,
46 Yun JW, Choi YO, Kim WY, Kang JS, Cheong GW, Yun DJ, Rhee SG, Cho
47 MJ, and Lee SY. Two enzymes in one; two yeast peroxiredoxins display
48 oxidative stress-dependent switching from a peroxidase to a molecular
49 chaperone function. *Cell*. 117:625-635, 2004.
50
51
52
53
54
55
56
57
58
59
60

- 1
2
3 23. Jeong W, Cha MK, and Kim IH. Thioredoxin-dependent hydroperoxide peroxidase
4 activity of bacterioferritin comigratory protein (BCP) as a new member of the
5 thiol-specific antioxidant protein (TSA)/Alkyl hydroperoxide peroxidase C
6 (AhpC) family. *J Biol Chem.* 275:2924-2930, 2000.
7
8
9
10
11 24. Kim H-Y, and Kim J-R. Thioredoxin as a reducing agent for mammalian
12 methionine sulfoxide reductases B lacking resolving cysteine. *Biochemical and*
13 *Biophysical Research Communications.* 371:490-494, 2008.
14
15
16
17 25. Kumar C, Igarria A, D'Autreaux B, Planson A-G, Junot C, Godat E,
18 Bachhawat AK, Delaunay-Moisan A, and Toledano MB. Glutathione revisited:
19 a vital function in iron metabolism and ancillary role in thiol-redox control. *The*
20 *EMBO Journal*, 2011.
21
22
23
24
25
26
27 26. Manevich Y, Feinstein SI, and Fisher AB. Activation of the antioxidant enzyme 1-
28 CYS peroxiredoxin requires glutathionylation mediated by heterodimerization
29 with pi GST. *Proc Natl Acad Sci U S A.* 101:3780-3785, 2004.
30
31
32
33
34 27. Monteiro G, Horta BB, Pimenta DC, Augusto O, and Netto LES. Reduction of 1-
35 Cys peroxiredoxins by ascorbate changes the thiol-specific antioxidant
36 paradigm, revealing another function of vitamin C. *Proceedings of the National*
37 *Academy of Sciences.* 104:4886-4891, 2007.
38
39
40
41
42
43 28. Noguera-Mazon V, Lemoine J, Walker O, Rouhier N, Salvador A, Jacquot JP,
44 Lancelin JM, and Krimm I. Glutathionylation induces the dissociation of 1-Cys
45 D-peroxiredoxin non-covalent homodimer. *J Biol Chem.* 281:31736-31742,
46 2006.
47
48
49
50
51 29. Park JW, Rhee SG, and Chock PB. Glutathionylation of Peroxiredoxin I Induces
52 Decamer to Dimers Dissociation with Concomitant Loss of Chaperone Activity.
53 *Biochemistry.* 50:3204-3210, 2011.
54
55
56
57
58
59
60

- 1
2
3 30. Pedrajas JR, Kosmidou E, Miranda-Vizuete A, Gustafsson JA, Wright AP, and
4
5 Spyrou G. Identification and functional characterization of a novel
6
7 mitochondrial thioredoxin system in *Saccharomyces cerevisiae*. *J. Biol. Chem.*
8
9 274:6366-6373., 1999.
10
11 31. Pedrajas JR, Miranda-Vizuete A, Javanmardy N, Gustafsson JA, and Spyrou G.
12
13 Mitochondria of *saccharomyces cerevisiae* contain one-conserved cysteine type
14
15 peroxiredoxin with thioredoxin peroxidase activity. *J. Biol. Chem.* 275:16296-
16
17 16301, 2000.
18
19 32. Pedrajas JR, Padilla CA, McDonagh B, and Barcena JA. Glutaredoxin participates
20
21 in the reduction of peroxides by the mitochondrial 1-CYS peroxiredoxin in
22
23 *Saccharomyces cerevisiae*. *Antioxidants & redox signaling.* 13:249-258, 2010.
24
25 33. Pedrajas JR, Porras P, Martinez-Galisteo E, Padilla CA, Miranda-Vizuete A, and
26
27 Barcena JA. Two isoforms of *Saccharomyces cerevisiae* glutaredoxin 2 are
28
29 expressed in vivo and localize to different subcellular compartments. *Biochem J.*
30
31 364:617-623, 2002.
32
33 34. Ralat LA, Misquitta SA, Manevich Y, Fisher AB, and Colman RF. Characterization
34
35 of the complex of glutathione S-transferase pi and 1-cysteine peroxiredoxin.
36
37 *Archives of Biochemistry and Biophysics.* 474:109-118, 2008.
38
39 35. Rodriguez-Manzaneque MT, Ros J, Cabiscol E, Sorribas A, and Herrero E. Grx5
40
41 glutaredoxin plays a central role in protection against protein oxidative damage
42
43 in *Saccharomyces cerevisiae*. *Mol Cell Biol.* 19:8180-8190, 1999.
44
45 36. Roy A, Kucukural A, and Zhang Y. I-TASSER: a unified platform for automated
46
47 protein structure and function prediction. *Nature Protocols.* 5:725-738, 2010.
48
49 37. Schilling B, Rardin MJ, MacLean BX, Zawadzka AM, Frewen BE, Cusack MP,
50
51 Sorensen DJ, Bereman MS, Jing E, Wu CC, Verdin E, Kahn CR, MacCoss MJ,
52
53
54
55
56
57
58
59
60

- 1
2
3 and Gibson BW. Platform-independent and Label-free Quantitation of
4 Proteomic Data Using MS1 Extracted Ion Chromatograms in Skyline:
5 APPLICATION TO PROTEIN ACETYLATION AND
6 PHOSPHORYLATION. *Molecular & Cellular Proteomics*. 11:202-214,
7 2012.
8
9
10
11
12
13
14 38. Sheehan D, Meade G, Foley VM, and Dowd CA. Structure, function and evolution
15 of glutathione transferases: implications for classification of non-mammalian
16 members of an ancient enzyme superfamily. *The Biochemical journal*. 360:1-16,
17 2001.
18
19
20
21
22
23 39. Soito L, Williamson C, Knutson ST, Fetrow JS, Poole LB, and Nelson KJ. PREX:
24 PeroxiRedoxin classification indEX, a database of subfamily assignments across
25 the diverse peroxiredoxin family. *Nucleic Acids Research*. 39:D332-D337, 2010.
26
27
28
29
30 40. Tarrago L, Laugier E, Zaffagnini M, Marchand C, Le Marechal P, Rouhier N,
31 Lemaire S, and Rey P. Regeneration mechanisms of Arabidopsis thaliana
32 methionine sulfoxide reductases B by glutaredoxins and thioredoxins. *Journal of*
33 *Biological Chemistry*. 284:18963-18971, 2009.
34
35
36
37
38 41. Tarrago L, Laugier E, Zaffagnini M, Marchand CH, Le Maréchal P, Lemaire SD,
39 and Rey P. Plant thioredoxin CDSP32 regenerates 1-cys methionine sulfoxide
40 reductase B activity through the direct reduction of sulfenic acid. *Journal of*
41 *Biological Chemistry*. 285:14964-14972, 2010.
42
43
44
45
46
47 42. Towbin H, Staehelin T, and Gordon J. Electrophoretic transfer of proteins from
48 polyacrylamide gels to nitrocellulose sheets: procedure and some applications.
49 *Proc. Natl. Acad. Sci. U. S. A.* 76:4350-4354, 1979.
50
51
52
53
54 43. Vögtle FN, Wortelkamp S, Zahedi RP, Becker D, Leidhold C, Gevaert K,
55 Kellermann J, Voos W, Sickmann A, Pfanner N, and Meisinger C. Global
56
57
58
59
60

1
2
3 Analysis of the Mitochondrial N-Proteome Identifies a Processing Peptidase
4
5 Critical for Protein Stability. *Cell*. 139:428-439, 2009.

6
7 44. Wood ZA, Poole LB, and Karplus PA. Peroxiredoxin evolution and the regulation
8
9 of hydrogen peroxide signaling. *Science*. 300:650-653, 2003.

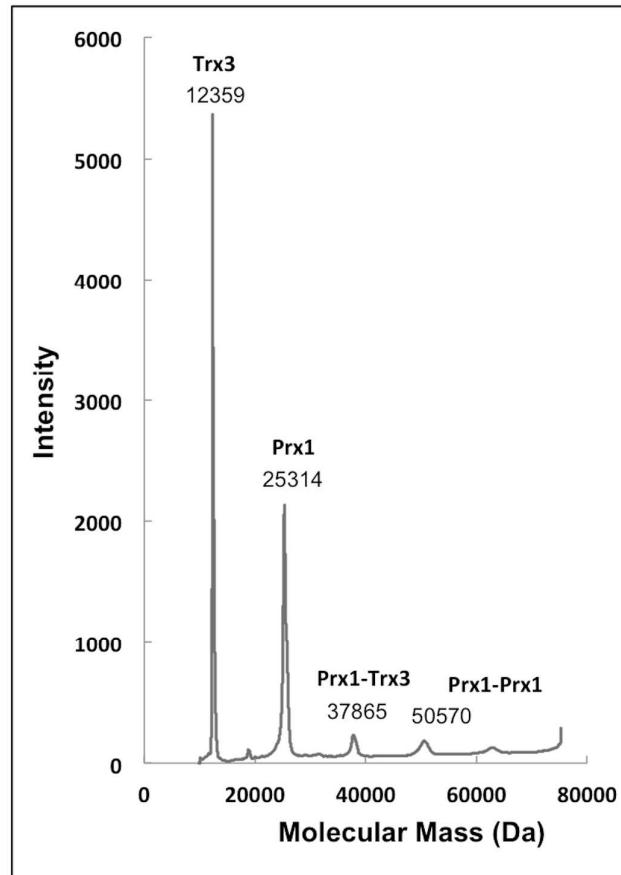
10
11 45. Yang J, Yan R, Roy A, Xu D, Poisson J, and Zhang Y. The I-TASSER Suite:
12
13 protein structure and function prediction. *Nature methods*. 12:7-8, 2015.
14
15
16
17
18
19
20
21
22
23
24
25
26
27
28
29
30
31
32
33
34
35
36
37
38
39
40
41
42
43
44
45
46
47
48
49
50
51
52
53
54
55
56
57
58
59
60

SUPPLEMENTAL DATA

Legend to Supplementary Figure

An incubation mixture containing 20 μM Prx1p and Thioredoxin System: TS: 50 μM NADPH, 0.5 μM Trr2p and 5 μM Trx3p was vacuum-dried, resuspended in 0.1% TFA and 1 μl was spotted onto a MALDI plate. When dried, 0.6 μl sinapinic acid (10mg/ml in 0.3% TFA, 30% AN) were added and let until crystallization. The molecular mass analysis was carried out in a ABSciex MALDI-TOF/TOF 5800 mass spectrometer. Data acquisition was done using a High Mass method in a mass range between 10 - 75 kDa and the focused mass was fixed at at 35 kDa. 7500 shots were directed to the sample with a fixed lasser intensity of 4800 and a speed of movement over the sample of 700 $\mu\text{m/s}$.

Supplementary figure



Legends to schemes and figures

Scheme 1: A) Catalytic cycle of Prx1p as deduced from the data presented in this study. Each Prx1p polypeptide is represented by a large “P” with their peroxidatic Cys91 highlighted in the different redox states: sulfhydryl –SH, sulfenic –SOH, disulfide –S-S- and glutathionylated –SSG. Each step of the catalytic cycle is indicated with a circled number from 1 to 3; numbers with grey shadow represent the most likely steps under normal physiological conditions with GSH playing a catalytic and protective role in the resolving step and the mitochondrial thioredoxin system contributing the reducing recycling step. For more details see the main text. **B)** GSH dependent recycling of Prx1p by Trx3p should take place through a dithiolic mechanism in which reduced Trx3p(SH)₂ would form a transient mixed disulfide with Prx1p. The mixed disulfide should be resolved by the second cysteine to recover GSH and producing oxidized Trx3p. Trx2p should eventually transfer reducing equivalents from NADPH to regenerate reduced Trx3p(SH)₂.

Figure 1: A) Alignment of Prx1 with human PRXD6; the sequences of the three sites that constitute the functional signature of Prx6 subfamily according to PREX are highlighted in three different colors. The two cleavage sites assumed to design the recombinant proteins N21Prx1p and N39Prx1p are marked. In recombinant N21(S)Prx1p Cys38 was substituted by Serine. **B)** Structural modeling of mature Prx1 (dark blue) using human PRXD6 (PDB: 1prx.A; green) as a template; the side chains of three consensus residues of the Prx6 subfamily signature underlined in B) are shown and the functional structural signatures are highlighted in the same colors as in B). **C)**

1
2
3 SDS-PAGE of N21Prx1p (a) and N21(S)Prx1p (b) denatured under reducing and non-
4
5 reducing conditions as described in Materials and Methods. The first lane contains Mw
6
7 markers as indicated. (*) Samples were preincubated with 1mM GSH before denaturing.
8
9 (To see this illustration in color the reader is referred to the web version of this article at
10
11 www.liebertonline.com/ars).

12
13
14
15
16 **Figure 2:** Non-reducing SDS-PAGE of N39Prx1p after various treatments. **A)** Samples
17
18 of 20 μM N39Prx1p pretreated with increasing concentrations of GSH (0-1000 μM). **B)**
19
20 Samples of 20 μM N39Prx1p untreated (-) or pretreated with 1mM GSH, 0.5mM
21
22 GSSG, a complete Thioredoxin System (TS), Thioredoxin System without Trx3p, 1mM
23
24 TCEP or 1mM ascorbate. The Thioredoxin System is composed of 0.25mM NADPH,
25
26 0.5 μM Trr2p and 2 μM Trx3p. **C)** 20 μM N39Prx1p untreated (-); or pre-treated first
27
28 with 0.1mM TCEP followed by 0, 10, 20, 40, 60, 80, 100, 250 y 500 μM H_2O_2 . The
29
30 graphic shows a densitometry from the image of the bands corresponding to 56 kDa
31
32 (black bars) and 28 kDa (grey bars). **D)** 20 μM N39Prx1p pre-incubated with a
33
34 Thioredoxin System (TS) followed by addition of a Peroxide Generating System (PGS).
35
36 Aliquots were taken from the incubation mixture at the indicated times, were denatured
37
38 without reductant and loaded onto SDS-PAGE; **E)** same as in D), but with 100 μM GSH
39
40 added to the TS. TS: 50 μM NADPH, 0.5 μM Trr2p and 5 μM Trx3p; PGS: 1mM
41
42 xantine, 50mU xantine oxidase and 12U SOD.
43
44
45
46
47
48

49
50 **Figure 3:** **A)** Western blot of N39Prx1 showing in the left panel the Coomassie blue
51
52 staining of a SDS-PAGE; sample 1 was denatured under standard reducing conditions
53
54 and samples 2-4 under non-reducing conditions. Samples 3 and 4 were pre-treated with
55
56 1mM GSH or 0.1 mM TCEP, respectively, before denaturing. The bands **a** to **d** were
57
58
59
60

1
2
3 picked for the mass spectrometry analysis; the right panel shows the Western blot of
4
5 those samples with specific anti-GSH antibody. **B)** De glutathionylase activity of Trx3p.
6
7 20 μM N39Prx1p samples pre-incubated or not with 0.5 mM GSH for 30 min as
8
9 indicated, and then either treated or not with a mitochondrial thioredoxin reducing
10
11 system, were subjected to non-reducing SDS-PAGE and then analyzed by Western blot
12
13 with anti-GSH antibodies. Ponceau red stained membrane and developing with specific
14
15 anti-GSH antibodies are shown. Mw markers were loaded on the first lane. The
16
17 Thioredoxin System consisted of 250 μM NADPH, 0.5 μM Trr2p and 5 μM Trx3p. **C)**
18
19 the protein bands a-d shown in A) were picked, digested with AspN proteinase and
20
21 analyzed by LC-MS/MS. The MS/MS spectrum of glutathionylated 86-105 peptide
22
23 identified in band **c** is shown; the detected fragment ions of the *y* and *b* series are
24
25 indicated; Ions y_{15}^{2+} , y_{17}^{2+} and y_{18}^{2+} , which are exclusive of the glutathionylated peptide,
26
27 are conspicuous. **D)** Abundance of several redox modifications of the Cys91 containing
28
29 peptide were measured and are shown in arbitrary units.
30
31
32
33
34
35

36 **Figure 4:** **A)** Analysis of 20 μM samples of N39Prx1p by size exclusion
37
38 chromatography without treatment (chromatogram a) or pre-treated with 1mM GSH
39
40 (chromatogram b). Numbered arrows indicate the elution times of Mw markers: 1, Blue
41
42 dextran (2.000 kDa); 2, ferritin (450 kDa); 3, alcohol dehydrogenase (150 kDa); 4,
43
44 bovine serum albumin (66 kDa); 5, carbonic anhydrase (29 kDa). F1 and F2 indicate
45
46 fractions collected during the marked time intervals from chromatographies a and b,
47
48 respectively. Inset, non-reducing SDS-PAGE of those fractions. **B)** Size exclusion
49
50 chromatographies of cell-free extracts from WT (green line) and ΔPRX1 (purple line)
51
52 yeast. Grey lines are the elution profiles of recombinant N39Prx1p shown in A) here
53
54
55
56
57
58
59
60

1
2
3 superimposed for comparison. Fractions from both samples, as indicated, were collected
4
5 and analyzed by Western blot with anti-Prx1 antibody (right panel).
6
7
8

9
10 **Figure 5:** Detection of Prx1p in cell-free extracts from different yeast strains. **A)** The
11 extracts were denatured under non-reducing conditions and 12.5 μ g protein aliquots
12 were analyzed by Western blot. **B)** Same as in A) but the extracts were further dialyzed
13 at 4°C overnight. The migration positions of Mw markers are shown.
14
15
16
17
18

19
20 **Figure 6:** Thioredoxin peroxidase activity of N39Prx1p. The standard thioredoxin
21 peroxidase assay was performed as described in Materials and Methods. At the time
22 indicated by an arrow was added 1mM H₂O₂. **A)** The decrease in absorbance at 340 nm
23 due to NADPH oxidation was recorded along time in an assay without Trx3p (upper
24 line); in a normal standard assay (lower line); without GSH as indicated; and with GSH
25 added at the time indicated by an arrow. **B)** The activity was measured without GSH,
26 but at the times indicated by the arrows 0.5mM GSH was added to the reaction mixture,
27 the reaction progress was monitored and the initial rates are shown in the inserted table.
28
29 **C)** Thioredoxin peroxidase activities at different GSH concentrations. The inset is a
30 double reciprocal plot from the data at the lower concentrations, which indicated an
31 apparent Km of 6.1 μ M for GSH. **D)** Peroxidase activity of N39Prx1p dependent on
32 Grx2p. The composition of the assay was as described in Materials and Methods.
33
34
35
36
37
38
39
40
41
42
43
44
45
46
47
48

49 **Figure 7: A)** Predicted positions of GSH (purple) docked on a model of Prx1p (green)
50 around the active site Cys91. Side-chains of residues from the catalytic triad according
51 to PREX are shown. Arg175 and its distance to Cys91 are also depicted. The distance
52 between Cys91 and GSH is also shown. **B)** and **C)** structure of dimeric human PRXD6
53
54
55
56
57
58
59
60

1
2
3 (PDB, 1prx). The surface of each subunit is colored differently; Cys47 from the yellow
4 subunit is shown in purple color in B). C) Space filling of a wide and long groove in the
5 interphase around Cys47 is shown in purple color in B). C) Space filling of a wide and long groove in the
6 interphase around Cys47 is shown in purple color in B). C) Space filling of a wide and long groove in the
7 interphase around Cys47 is shown in purple color in B). C) Space filling of a wide and long groove in the
8 interphase around Cys47 is shown in purple color in B). C) Space filling of a wide and long groove in the
9 interphase around Cys47 is shown in purple color in B). C) Space filling of a wide and long groove in the
10 interphase around Cys47 is shown in purple color in B). C) Space filling of a wide and long groove in the
11 interphase around Cys47 is shown in purple color in B). C) Space filling of a wide and long groove in the
12 interphase around Cys47 is shown in purple color in B). C) Space filling of a wide and long groove in the
13 interphase around Cys47 is shown in purple color in B). C) Space filling of a wide and long groove in the
14 interphase around Cys47 is shown in purple color in B). C) Space filling of a wide and long groove in the
15 interphase around Cys47 is shown in purple color in B). C) Space filling of a wide and long groove in the
16 interphase around Cys47 is shown in purple color in B). C) Space filling of a wide and long groove in the
17 interphase around Cys47 is shown in purple color in B). C) Space filling of a wide and long groove in the
18 interphase around Cys47 is shown in purple color in B). C) Space filling of a wide and long groove in the
19 interphase around Cys47 is shown in purple color in B). C) Space filling of a wide and long groove in the
20 interphase around Cys47 is shown in purple color in B). C) Space filling of a wide and long groove in the
21 interphase around Cys47 is shown in purple color in B). C) Space filling of a wide and long groove in the
22 interphase around Cys47 is shown in purple color in B). C) Space filling of a wide and long groove in the
23 interphase around Cys47 is shown in purple color in B). C) Space filling of a wide and long groove in the
24 interphase around Cys47 is shown in purple color in B). C) Space filling of a wide and long groove in the
25 interphase around Cys47 is shown in purple color in B). C) Space filling of a wide and long groove in the
26 interphase around Cys47 is shown in purple color in B). C) Space filling of a wide and long groove in the
27 interphase around Cys47 is shown in purple color in B). C) Space filling of a wide and long groove in the
28 interphase around Cys47 is shown in purple color in B). C) Space filling of a wide and long groove in the
29 interphase around Cys47 is shown in purple color in B). C) Space filling of a wide and long groove in the
30 interphase around Cys47 is shown in purple color in B). C) Space filling of a wide and long groove in the
31 interphase around Cys47 is shown in purple color in B). C) Space filling of a wide and long groove in the
32 interphase around Cys47 is shown in purple color in B). C) Space filling of a wide and long groove in the
33 interphase around Cys47 is shown in purple color in B). C) Space filling of a wide and long groove in the
34 interphase around Cys47 is shown in purple color in B). C) Space filling of a wide and long groove in the
35 interphase around Cys47 is shown in purple color in B). C) Space filling of a wide and long groove in the
36 interphase around Cys47 is shown in purple color in B). C) Space filling of a wide and long groove in the
37 interphase around Cys47 is shown in purple color in B). C) Space filling of a wide and long groove in the
38 interphase around Cys47 is shown in purple color in B). C) Space filling of a wide and long groove in the
39 interphase around Cys47 is shown in purple color in B). C) Space filling of a wide and long groove in the
40 interphase around Cys47 is shown in purple color in B). C) Space filling of a wide and long groove in the
41 interphase around Cys47 is shown in purple color in B). C) Space filling of a wide and long groove in the
42 interphase around Cys47 is shown in purple color in B). C) Space filling of a wide and long groove in the
43 interphase around Cys47 is shown in purple color in B). C) Space filling of a wide and long groove in the
44 interphase around Cys47 is shown in purple color in B). C) Space filling of a wide and long groove in the
45 interphase around Cys47 is shown in purple color in B). C) Space filling of a wide and long groove in the
46 interphase around Cys47 is shown in purple color in B). C) Space filling of a wide and long groove in the
47 interphase around Cys47 is shown in purple color in B). C) Space filling of a wide and long groove in the
48 interphase around Cys47 is shown in purple color in B). C) Space filling of a wide and long groove in the
49 interphase around Cys47 is shown in purple color in B). C) Space filling of a wide and long groove in the
50 interphase around Cys47 is shown in purple color in B). C) Space filling of a wide and long groove in the
51 interphase around Cys47 is shown in purple color in B). C) Space filling of a wide and long groove in the
52 interphase around Cys47 is shown in purple color in B). C) Space filling of a wide and long groove in the
53 interphase around Cys47 is shown in purple color in B). C) Space filling of a wide and long groove in the
54 interphase around Cys47 is shown in purple color in B). C) Space filling of a wide and long groove in the
55 interphase around Cys47 is shown in purple color in B). C) Space filling of a wide and long groove in the
56 interphase around Cys47 is shown in purple color in B). C) Space filling of a wide and long groove in the
57 interphase around Cys47 is shown in purple color in B). C) Space filling of a wide and long groove in the
58 interphase around Cys47 is shown in purple color in B). C) Space filling of a wide and long groove in the
59 interphase around Cys47 is shown in purple color in B). C) Space filling of a wide and long groove in the
60 interphase around Cys47 is shown in purple color in B). C) Space filling of a wide and long groove in the

interphase around Cys47 is shown in green. **D)** A closer look with GSH docked on the groove next to the catalytic site, where residues of the catalytic triad are shown. In this structure, Cys47 is oxidized in the form of -SOH and the active site is in the fully folded (FF) conformation. (To see this illustration in color the reader is referred to the web version of this article at www.liebertonline.com/ars).

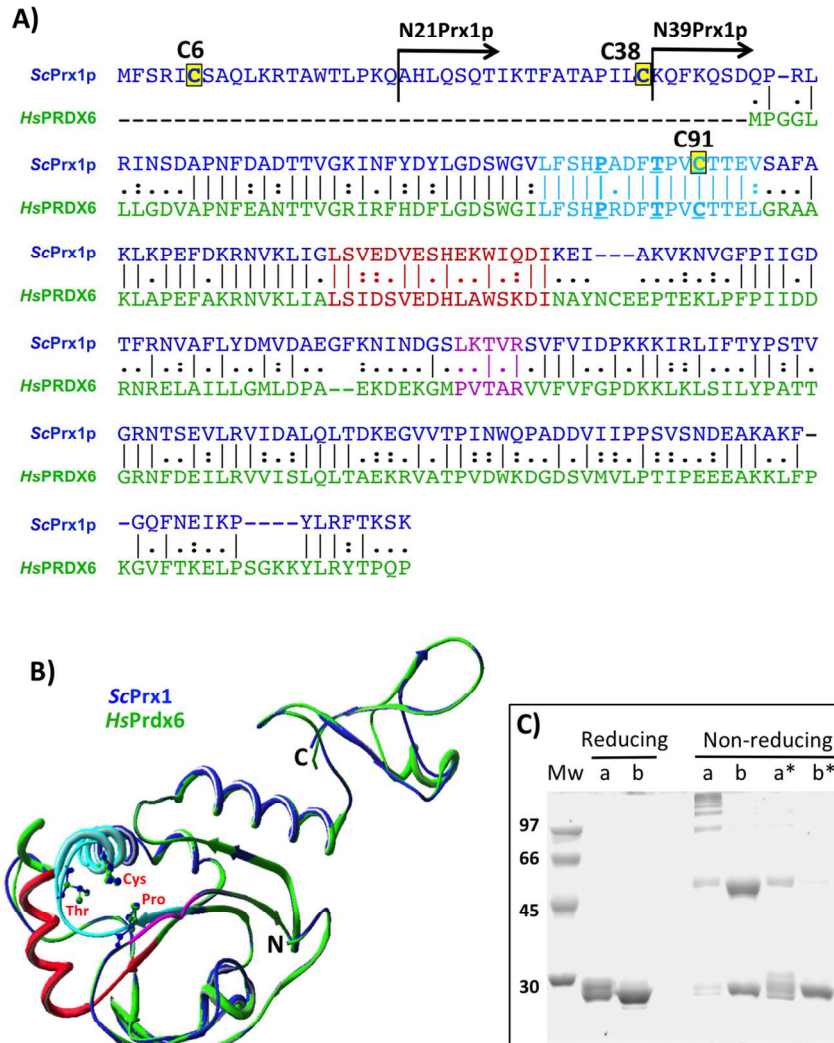


Figure 1: A) Alignment of Prx1 with human PRXD6; the sequences of the three sites that constitute the functional signature of Prx6 subfamily according to PREX are highlighted in three different colors. The two cleavage sites assumed to design the recombinant proteins N21Prx1p and N39Prx1p are marked. In recombinant N21(S)Prx1p Cys38 was substituted by Serine. B) Structural modeling of mature Prx1 (dark blue) using human PRXD6 (PDB: 1prx.A; green) as a template; the side chains of three consensus residues of the Prx6 subfamily signature underlined in B) are shown and the functional structural signatures are highlighted in the same colors as in B). C) SDS-PAGE of N21Prx1p (a) and N21(S)Prx1p (b) denatured under reducing and non-reducing conditions as described in Materials and Methods. The first lane contains Mw markers as indicated. (*) Samples were preincubated with 1mM GSH before denaturing. (To see this illustration in color the reader is referred to the web version of this article at www.liebertonline.com/ars). 423x564mm (72 x 72 DPI)

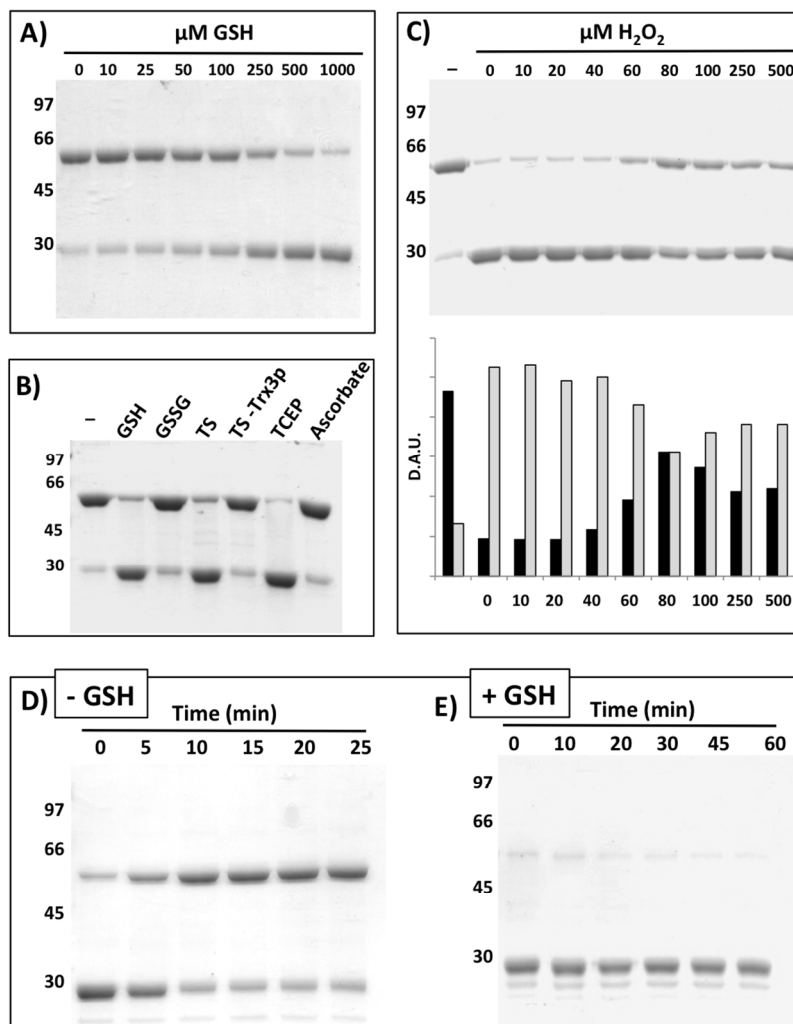


Figure 2: Non-reducing SDS-PAGE of N39Prx1p after various treatments. A) Samples of 20 μM N39Prx1p pretreated with increasing concentrations of GSH (0-1000 μM). B) Samples of 20 μM N39Prx1p untreated (-) or pretreated with 1mM GSH, 0.5mM GSSG, a complete Thioredoxin System (TS), Thioredoxin System without Trx3p, 1mM TCEP or 1mM ascorbate. The Thioredoxin System is composed of 0.25mM NADPH, 0.5 μM Trr2p and 2 μM Trx3p. C) 20 μM N39Prx1p untreated (-); or pre-treated first with 0.1mM TCEP followed by 0, 10, 20, 40, 60, 80, 100, 250 y 500 μM H₂O₂. The graphic shows a densitometry from the image of the bands corresponding to 56 kDa (black bars) and 28 kDa (grey bars). D) 20 μM N39Prx1p pre-incubated with a Thioredoxin System (TS) followed by addition of a Peroxide Generating System (PGS). Aliquots were taken from the incubation mixture at the indicated times, were denatured without reductant and loaded onto SDS-PAGE; E) same as in D), but with 100 μM GSH added to the TS. TS: 50 μM NADPH, 0.5 μM Trr2p and 5 μM Trx3p; PGS: 1mM xantine, 50mU xantine oxidase and 12U SOD. 423x564mm (72 x 72 DPI)

1
2
3
4
5
6
7
8
9
10
11
12
13
14
15
16
17
18
19
20
21
22
23
24
25
26
27
28
29
30
31
32
33
34
35
36
37
38
39
40
41
42
43
44
45
46
47
48
49
50
51
52
53
54
55
56
57
58
59
60

CONFIDENTIAL - For Peer Review Only

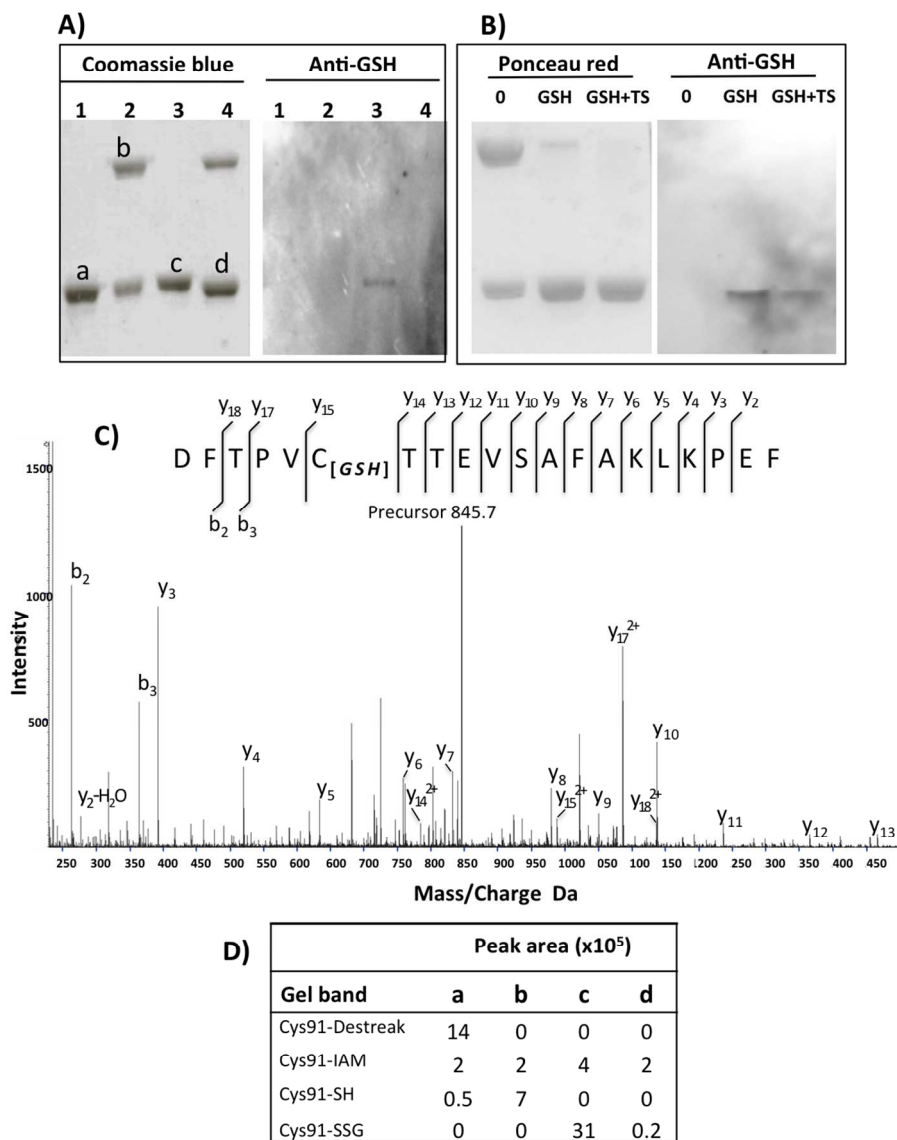


Figure 3: A) Western blot of N39Prx1 showing in the left panel the Coomassie blue staining of a SDS-PAGE; sample 1 was denatured under standard reducing conditions and samples 2-4 under non-reducing conditions. Samples 3 and 4 were pre-treated with 1mM GSH or 0.1 mM TCEP, respectively, before denaturing. The bands a to d were picked for the mass spectrometry analysis; the right panel shows the Western blot of those samples with specific anti-GSH antibody. B) Deglutathionylase activity of Trx3p. 20 μ M N39Prx1p samples pre-incubated or not with 0.5 mM GSH for 30 min as indicated, and then either treated or not with a mitochondrial thioredoxin reducing system, were subjected to non-reducing SDS-PAGE and then analyzed by Western blot with anti-GSH antibodies. Ponceau red stained membrane and developing with specific anti-GSH antibodies are shown. Mw markers were loaded on the first lane. The Thioredoxin System consisted of 250 μ M NADPH, 0.5 μ M Trx2p and 5 μ M Trx3p. C) the protein bands a-d shown in A) were picked, digested with AspN proteinase and analyzed by LC-MS/MS. The MS/MS spectrum of glutathionylated 86-105 peptide identified in band c is shown; the detected fragment ions of the y and b series are indicated; Ions y₁₅²⁺, y₁₇²⁺ and y₁₈²⁺, which are exclusive of the glutathionylated peptide, are conspicuous. D) Peak area (x10⁵) for different gel bands.

Abundance of several redox modifications of the Cys91 containing peptide were measured and are shown in arbitrary units.
423x564mm (72 x 72 DPI)

CONFIDENTIAL - For Peer Review Only

1
2
3
4
5
6
7
8
9
10
11
12
13
14
15
16
17
18
19
20
21
22
23
24
25
26
27
28
29
30
31
32
33
34
35
36
37
38
39
40
41
42
43
44
45
46
47
48
49
50
51
52
53
54
55
56
57
58
59
60

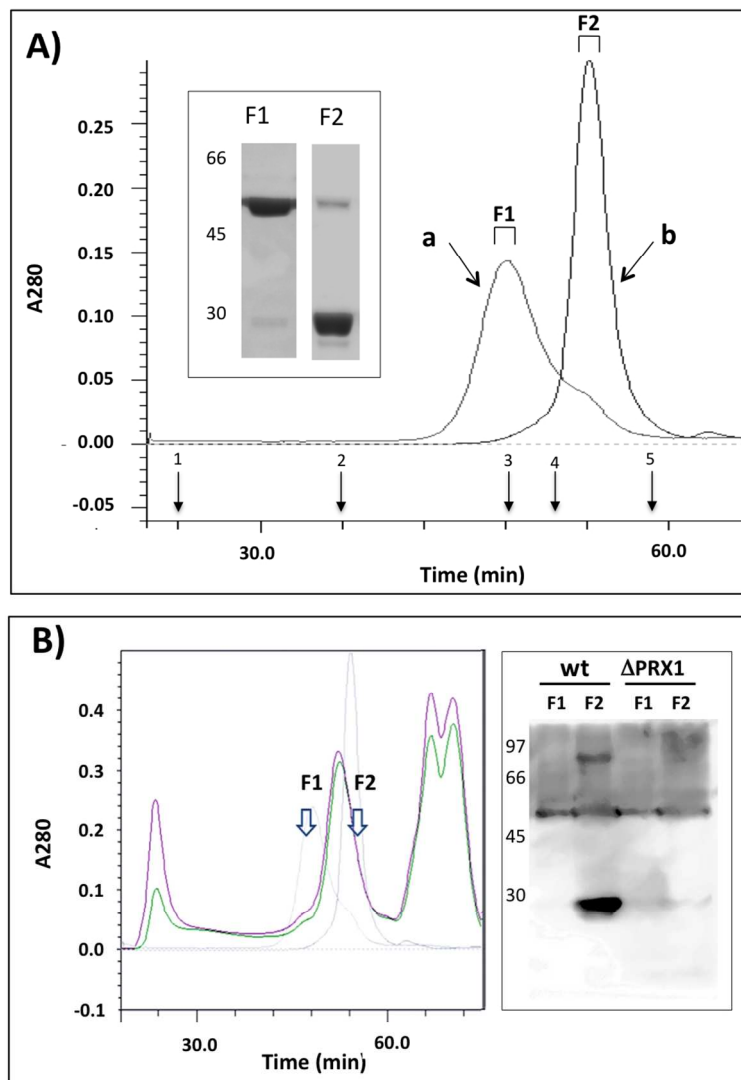


Figure 4: A) Analysis of 20 μM samples of N39Prx1p by size exclusion chromatography without treatment (chromatogram a) or pre-treated with 1mM GSH (chromatogram b). Numbered arrows indicate the elution times of Mw markers: 1, Blue dextran (2.000 kDa); 2, ferritin (450 kDa); 3, alcohol dehydrogenase (150 kDa); 4, bovine serum albumin (66 kDa); 5, carbonic anhydrase (29 kDa). F1 and F2 indicate fractions collected during the marked time intervals from chromatographies a and b, respectively. Inset, non-reducing SDS-PAGE of those fractions. B) Size exclusion chromatographies of cell-free extracts from WT (green line) and ΔPRX1 (purple line) yeast. Grey lines are the elution profiles of recombinant N39Prx1p shown in A) here superimposed for comparison. Fractions from both samples, as indicated, were collected and analyzed by Western blot with anti-Prx1 antibody (right panel).

423x564mm (72 x 72 DPI)

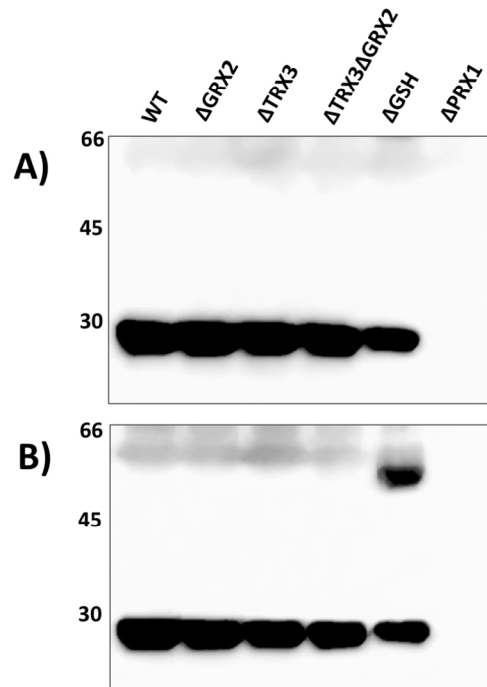


Figure 5: Detection of Prx1p in cell-free extracts from different yeast strains. A) The extracts were denatured under non-reducing conditions and 12.5 μ g protein aliquots were analyzed by Western blot. B) Same as in A) but the extracts were further dialyzed at 4°C overnight. The migration positions of Mw markers are shown.

423x564mm (72 x 72 DPI)

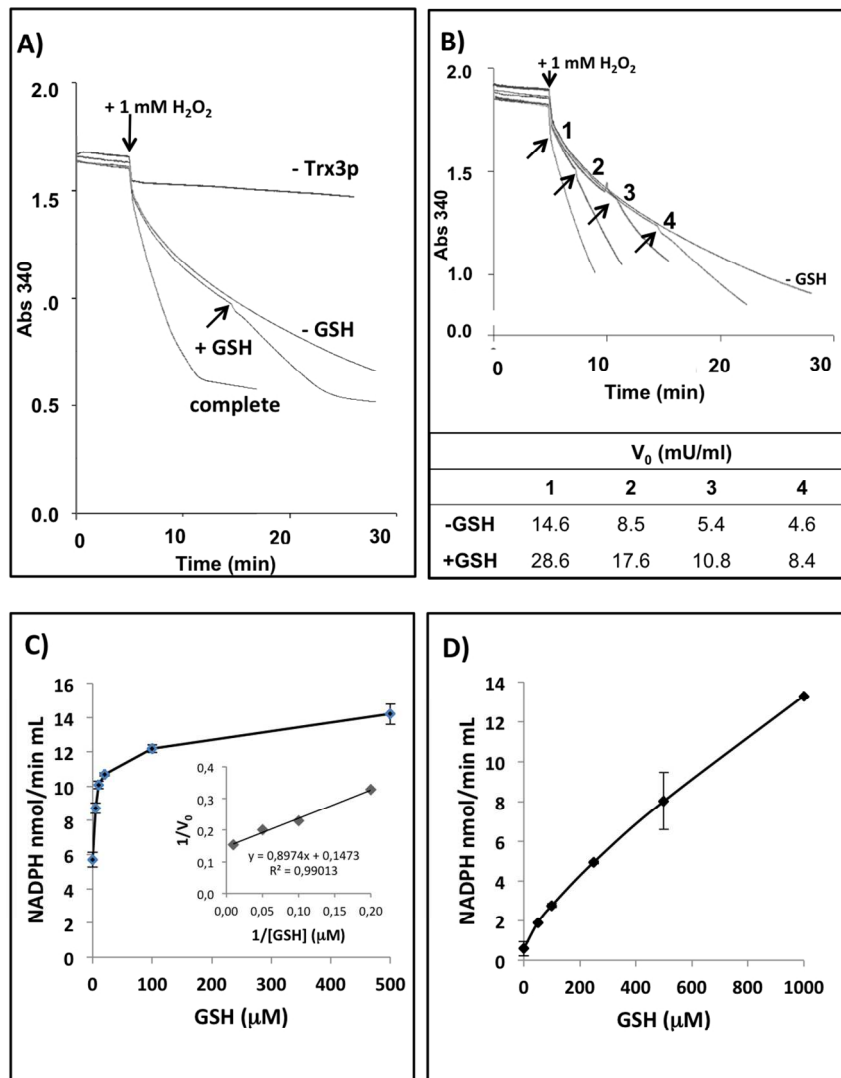


Figure 6: Thioredoxin peroxidase activity of N39Prx1p. The standard thioredoxin peroxidase assay was performed as described in Materials and Methods. At the time indicated by an arrow was added 1mM H₂O₂.

A) The decrease in absorbance at 340 nm due to NADPH oxidation was recorded along time in an assay without Trx3p (upper line); in a normal standard assay (lower line); without GSH as indicated; and with GSH added at the time indicated by an arrow. B) The activity was measured without GSH, but at the times indicated by the arrows 0.5mM GSH was added to the reaction mixture, the reaction progress was monitored and the initial rates are shown in the inserted table. C) Thioredoxin peroxidase activities at different GSH concentrations. The inset is a double reciprocal plot from the data at the lower concentrations, which indicated an apparent K_m of 6.1 μM for GSH. D) Peroxidase activity of N39Prx1p dependent on Grx2p.

The composition of the assay was as described in Materials and Methods.

423x564mm (72 x 72 DPI)

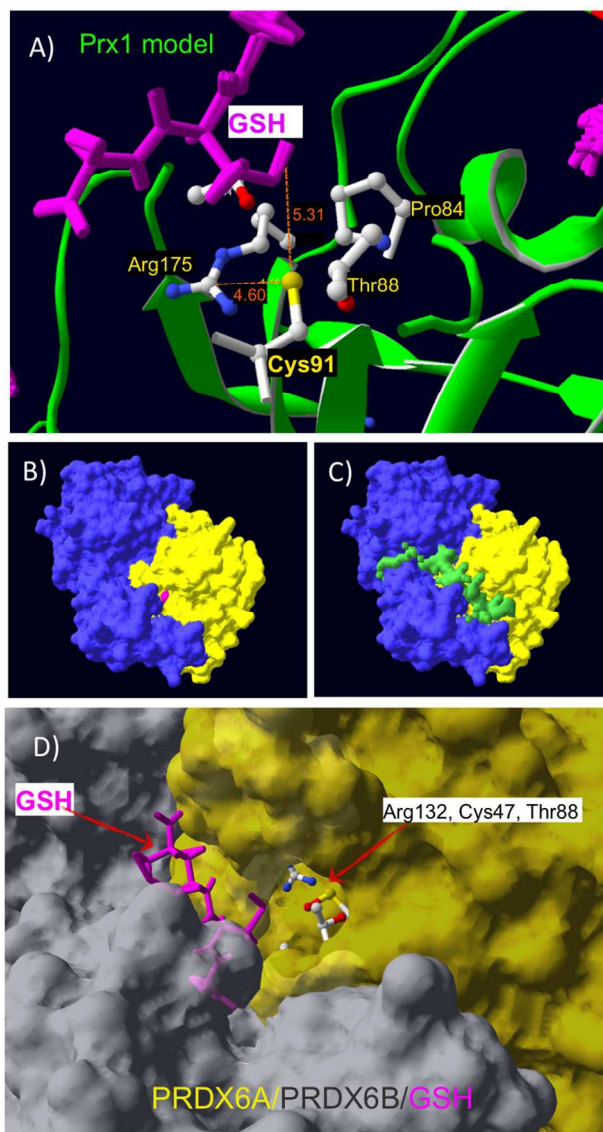
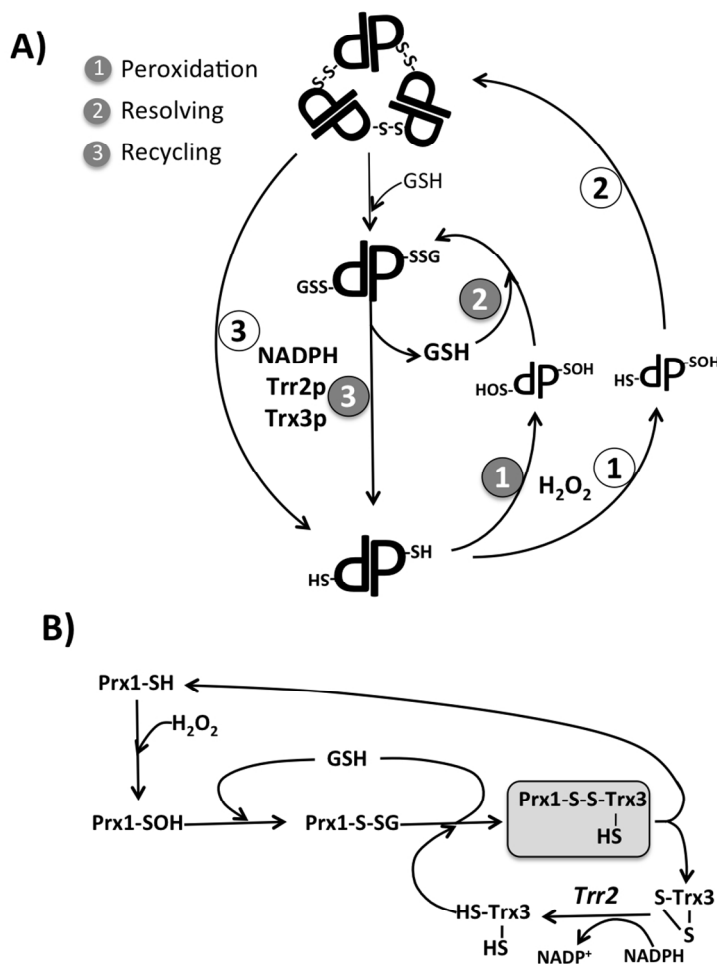


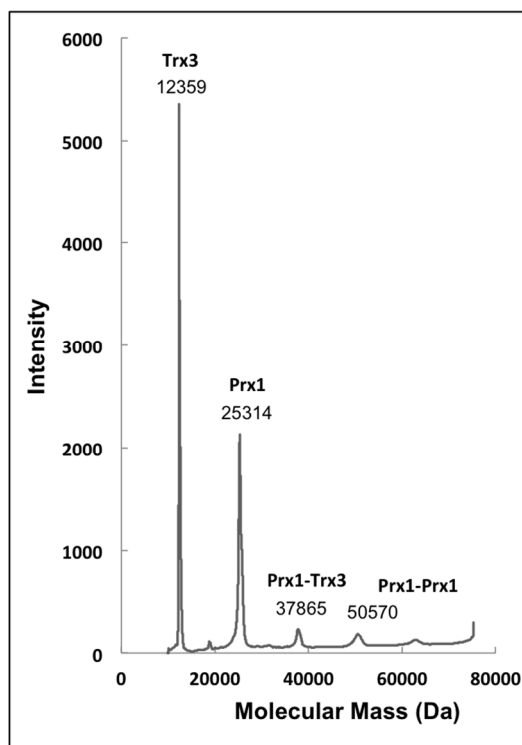
Figure 7: A) Predicted positions of GSH (purple) docked on a model of Prx1p (green) around the active site Cys91. Side-chains of residues from the catalytic triad according to PREX are shown. Arg175 and its distance to Cys91 are also depicted. The distance between Cys91 and GSH is also shown. B) and C) structure of dimeric human PRXD6 (PDB, 1prx). The surface of each subunit is colored differently; Cys47 from the yellow subunit is shown in purple color in B). C) Space filling of a wide and long groove in the interphase around Cys47 is shown in green. D) A closer look with GSH docked on the groove next to the catalytic site, where residues of the catalytic triad are shown. In this structure, Cys47 is oxidized in the form of -SOH and the active site is in the fully folded (FF) conformation. (To see this illustration in color the reader is referred to the web version of this article at www.liebertonline.com/ars).

423x564mm (72 x 72 DPI)



Scheme 1: A) Catalytic cycle of Prx1p as deduced from the data presented in this study. Each Prx1p polypeptide is represented by a large "P" with their peroxidatic Cys91 highlighted in the different redox states: sulfhydryl -SH, sulfenic -SOH, disulfide -S-S- and glutathionylated -SSG. Each step of the catalytic cycle is indicated with a circled number from 1 to 3; numbers with grey shadow represent the most likely steps under normal physiological conditions with GSH playing a catalytic and protective role in the resolving step and the mitochondrial thioredoxin system contributing the reducing recycling step. For more details see the main text. B) GSH dependent recycling of Prx1p by Trx3p should take place through a dithiolic mechanism in which reduced Trx3p(SH)₂ would form a transient mixed disulfide with Prx1p. The mixed disulfide should be resolved by the second cysteine to recover GSH and producing oxidized Trx3p. Trr2p should eventually transfer reducing equivalents from NADPH to regenerate reduced Trx3p(SH)₂.

423x564mm (72 x 72 DPI)



Legend to Supplementary Figure

An incubation mixture containing 20 μM Prx1p and Thioredoxin System: TS: 50 μM NADPH, 0.5 μM Trx2p and 5 μM Trx3p was vacuum-dried, resuspended in 0.1% TFA and 1 μl was spotted onto a MALDI plate. When dried, 0.6 μl sinapinic acid (10mg/ml in 0.3% TFA, 30% AN) were added and let until crystallization. The molecular mass analysis was carried out in a ABSciex MALDI-TOF/TOF 5800 mass spectrometer. Data acquisition was done using a High Mass method in a mass range between 10 - 75 kDa and the focused mass was fixed at at 35 kDa. 7500 shots were directed to the sample with a fixed lasser intensity of 4800 and a speed of movement over the sample of 700 $\mu\text{m/s}$.

423x564mm (72 x 72 DPI)